

Statistical Interference Modeling and Coexistence Strategies in Cognitive Wireless
Networks

A dissertation submitted in partial fulfillment of the requirements for the degree of
Doctor of Philosophy at George Mason University

By

Alireza Babaei
Master of Science
Iran University of Science and Technology, 2005
Bachelor of Science
K. N. Toosi University of Technology, 2003

Director: Dr. Bijan Jabbari, Professor
Department of Electrical and Computer Engineering

Spring Semester 2009
George Mason University
Fairfax, VA

Copyright © 2009 by Alireza Babaei
All Rights Reserved

Acknowledgments

I would like to extend my earnest appreciation to my family, especially my parents, for their continual stream of love and support. The blessing they have given throughout the years, has always been the most valuable asset in my life.

I would particularly like to express sincere gratitude to my advisor, Dr. Bijan Jabbari, for his support, guidance and encouragement throughout these three years. This was a unique opportunity and priceless experience for me to work with him.

I thank Dr. Shih-chun Chang, Dr. Yariv Ephraim, Dr. Jill Nelson and Dr. Robert Simon for serving on my committee. I would like to thank Dr. Chang for his insightful remarks. His expression of freedom along with the excellency in knowledge has been a source of inspiration for me.

My special thanks go to my good friends Hossein Roufarshbaf and Zeynab Masoudnia for their support and friendship during these years. I am thankful to all of my friends at Communications and Networking Lab. This was a great opportunity for me to work with and learn from these smart people from all around the world. I also thank Dr. Sun Y. Jung for her encouragement and bringing the spirit of art to our lab and reminding us to the more sunny side of the life. Thank you Sunny!

Table of Contents

	Page
List of Figures	vi
Abstract	viii
1 Introduction and Motivation	1
1.1 Spectrum Scarcity or Shortage of Tolerance?	1
1.2 Dynamic Spectrum Access and Cognitive Radios	2
1.3 Interference: The Achilles' Heel	3
1.4 Interference Modeling	5
1.4.1 Modeling of Cognitive Wireless Networks	6
1.4.2 Stochastic Geometry for Modeling the Coexisting Networks	6
1.5 Outline and Contribution of Dissertation	7
2 Distances in Spatial Point Processes	9
2.1 Spatial Point Processes With Single-Type Points	9
2.1.1 Spatial Poisson Point Processes	10
2.1.2 Spatial Binomial Point Processes	11
2.2 Spatial Bivariate Poisson Processes	12
2.2.1 Distance to n th Nearest Neighbor Distribution	15
2.2.2 Distance between type-B neighbors of a type-A point	23
3 Interference Modeling in Cognitive Wireless Networks	31
3.1 System Model	31
3.2 Interference Characterization	32
3.3 Approximation as a Normal Random Variable	34
3.3.1 Upper bound for $\text{var}\{I\}$	35
3.4 Approximation as the Sum of a Normal and Log-normal Random Variables	36
3.4.1 Bounds for s_1^2	39
3.4.2 CCDF of I	40
3.4.3 Approach one	41
3.4.4 Approach two	43
3.5 Interference Modeling with Traffic Considerations	46

3.5.1	Interference as a Normal Random Process	47
3.5.2	Sum of Normal and Log-normal Assumption	48
3.6	Simulation Results	50
4	Power Control for Interference Avoidance in Cognitive Wireless Networks	53
4.1	Aggregate interference as a Normal Random Variable	53
4.1.1	Power Control with Constant Power Levels	55
4.1.2	Power Control with Distance-dependent Power Levels	56
4.2	Aggregate Interference as Sum of a Normal and Log-normal Random Variables	59
4.2.1	Fixed Power Levels	60
4.2.2	Distance-dependent Power Levels	60
4.3	Power Control with Traffic Considerations	61
4.3.1	Interference as a Normal Random Process	61
4.3.2	Sum of Normal and Log-normal Assumption	62
4.4	Simulation Results	62
5	Achievable Throughput in Power-Constrained Cognitive Wireless Networks . . .	68
5.1	Achievable Throughput	68
5.2	Forwarding Strategy in Secondary Network	71
5.2.1	Nearest Neighbor Forwarding	71
5.2.2	Forwarding based on a distribution	72
5.3	Further Remarks	72
5.4	Simulation Results	74
6	Summary, Conclusions, and Future Work	75
6.1	Summary	75
6.2	Conclusions	76
6.3	Future Work	77
	Bibliography	78

List of Figures

Figure	Page
2.1 A sample 2-D spatial Poisson process with intensity $\lambda = 1$ where points are distributed in a disc of radius 5.	11
2.2 node i is the i th nearest type-B neighbor of a type-A point. node jk is the k th nearest type-B neighbor of node j	16
2.3 Conditional intensity of type-B points given a type-A point exists at the origin ($\lambda = 1$, $\mu = 2$, and $\sigma^2 = 0.5$).	19
2.4 $f_{r_{AB}}(r)$ ($\lambda = 1$, $\mu = 2$, and $\sigma^2 = 0.1$).	20
2.5 $E\{r_{AB}\}$ ($\lambda = 1$, $\mu = 2$, and $\sigma^2 = 0.1$).	21
2.6 Normalized histogram and analytical pdf of φ_{ij} ($i = 10$ and $j = 20$).	28
2.7 Normalized histogram of θ_{ijk} and uniform pdf ($i = 10$, $j = 20$ and $k = 5$).	29
2.8 Simulation (statistical mean) and analytical result for $E\{R_{AB,n}^\alpha\}$	29
2.9 Simulation (statistical mean) and analytical result for $E\{R_{ij}^\alpha\}$ ($i = 10$ and $j = 20$)	30
2.10 Simulation (statistical mean) and analytical result for $E\{d_{ijk}^\alpha\}$ ($i = 10$, $j = 20$ and $k = 5$)	30
3.1 Aggregated interference from secondary network to a primary node.	32
3.2 Convexity of $Q(\frac{\eta - \mu_2 - x}{\sigma_2})$	43
3.3 Normalized histogram of $I = \sum_{i=1}^{\infty} \xi_i R_{P_{S,i}}^\alpha$ and the pdf of the $\mathcal{N}(E\{I\}, V)$	51
3.4 The normalized histogram of $I_1 = \sum_{i=1}^N \xi_i P_{S,i} R_{P_{S,i}}^\alpha$ for $P_{S,i} = p_1 = 1$, $N = 1000$ and $\alpha = -3.2$ and the pdfs of $\mathcal{LN}(\mu_{1,l}, \sigma_{1,l})$ and $\mathcal{LN}(\mu_{1,u}, \sigma_{1,u})$	51
3.5 Histogram of I_2 and the pdf of $\mathcal{N}(\mu_2, \sigma_2)$	52
4.1 The acceptable values for (C_2, k) in (4.12) to satisfy the interference constraint in Lemma 7 in Chapter 3.	58
4.2 Constant k in (4.12), when $C_2 = 0$, $\beta = -\alpha/2 - 1.1$ and for different values of path loss exponent ($\lambda = 1$, $\mu = 2$, $\nu = 0.5$, $\eta = 0$ dBm, and $\sigma^2 \gg 1$).	59

4.3	Average Power levels of the first 50 secondary neighbors chosen by the second power control strategy ($\alpha = -3, C_2 = 0$).	64
4.4	Average Aggregated interference from secondary network on the primary node with constant power-level power control strategy ($\eta = 0$ dBm).	65
4.5	Average Aggregated interference from secondary network on the primary node with distance-dependent power-level power control strategy ($\beta = -\alpha/2 - 1.1, \eta = 0$ dBm, $C_2 = 0$).	65
4.6	constant k in (4.12) when distance-dependent power control strategy is used and for different values of Π and Δ ($\alpha = -3.2, \beta = -\alpha/2 - 1.5 = 0.1, \eta = 0$ dBm, $\epsilon = 0.1, C_2 = 0$).	66
4.7	P_{exc} vs. Path Loss Exponent for power control strategy with fixed power levels. $p_1 = p_2$ are chosen such that Bound 1 or Bound 2 are satisfied. The threshold for P_{exc} , (i.e., ϵ) is set to 0.01 and $\eta = 1 \sim 0$ dBW.	66
4.8	P_{exc} vs. Path Loss Exponent for power control strategy with distance-dependent power levels. We have set $\beta = -\alpha/2 - 1.05$ (increasing power levels), and $k = p_1 N^{-\beta}$. p_1 is chosen such that Bound 1 or Bound 2 are satisfied.	67
4.9	Transmitted power level vs. Path Loss Exponent for power control strategy with fixed power levels ($p_1 = p_2$). $p_1 = p_2$ is chosen such that Bound 1 or Bound 2 are satisfied.	67
5.1	Lower-bound for $E\{C_j\}$, $j = 50$, versus path loss exponent, for constant and distance-dependent power control strategies and for uniform and nearest neighbor forwarding.	73
5.2	Lower-bound for $E\{C_j\}$, versus j ($10 < j \leq 100$ and $\alpha = -3.1$) for constant and distance-dependent power control strategies and for uniform and nearest neighbor forwarding.	73

Abstract

STATISTICAL INTERFERENCE MODELING AND COEXISTENCE STRATEGIES IN COGNITIVE WIRELESS NETWORKS

Alireza Babaei, PhD

George Mason University, 2009

Dissertation Director: Dr. Bijan Jabbari

Cognitive radio is a novel approach for better utilization of the scarce, already packed but highly underutilized radio spectrum. To this end, environment-aware unlicensed secondary wireless devices are envisioned to share the spectrum with the primary licensed network, provided that their operation does not impose unmanageable interference on the primary nodes.

To achieve this coexistence goal, interference modeling is of great significance. Interference, in general, has a stochastic nature not only due to randomness in the propagation channel, but also due to the random geographic dispersion of nodes. A statistical representation for interference, in which the power levels of the secondary nodes influence the parameters of the model, is, thus, of considerable interest in analysis and design of cognitive wireless network.

Stochastic geometry and spatial point processes are used for modeling the coexisting primary and secondary networks. In particular, we model these networks using spatial bivariate Poisson processes. We obtain statistical properties of the distances in these

processes and use them for modeling the interference from secondary network on the primary nodes. We first consider an approximate Gaussian model for interference assuming that Central Limit Theorem (C.L.T) can be applied. We, then, show that a more accurate model for interference is the sum of a Normal and a Log-normal random variables. The power levels of secondary nodes can be adjusted to obtain desirable values for the parameters in both of these models.

Having this characterization of interference, we propose power control strategies for the secondary network which assure the satisfaction of interference constraint at the primary nodes. We show that these strategies are very easy to implement with little coordination requirement. Nodes either need to know where they are located in the sequence of nodes ordered according to their Euclidean distance to a primary node or need no location information, based on which strategy is being used.

Given that secondary nodes have imposed power control strategies to coexist with the primary nodes, we find the lower bound of achievable throughput for the secondary nodes. We use the statistical properties of distances between secondary nodes and find an upper bound for the interference of secondary network on an arbitrary secondary node and thereby a lower bound for its throughput. We show that the approach is applicable to finding the throughput in a general power-constrained random network.

Chapter 1: Introduction and Motivation

1.1 Spectrum Scarcity or Shortage of Tolerance?

Today, we are witnessing an unprecedented growth in demand for wireless technology. Several novel applications requiring high bandwidth are increasing the demand for radio spectrum. The radio frequencies, once perceived as an abundant resource, has turned into a seemingly diminishing commodity. A brief look at the domestic and international frequency allocation charts may lead to the conclusion that we are actually approaching the capacity of radio spectrum.

As of late, the trend to increase spectral efficiency, has been at the system level. This means that, for an allocated frequency band to a particular system, the communications engineers try to take the most out of it, e.g., by closing the gap to Shannon capacity as much as possible. Despite tremendous advances in physical layer techniques for more efficient use of radio spectrum, the problem still remains intact: how can the emerging wireless applications be integrated in the current overly crowded radio spectrum? This necessitates, as a *sine qua non*, a new paradigm and a fundamental revision in approaching the spectrum scarcity problem.

According to the Federal Communication Commission (FCC), at a given geographic location, spectrum remains idle for a large portion of time [1]. This brings the following questions: 1) Is the problem really the *physical shortage of spectrum*, or the *outdated spectrum policies* that prevent the coexistence? and 2) Can the efficiency of spectrum access be increased by allowing several systems coexist in the same frequency band?

In the traditional *divide and set aside* approach [2], service providers are granted blocks of spectrum along with licenses with which they can have exclusive access to the spectrum.

When licensees are not transmitting, the spectrum remains idle. These policies were devised considering the 1920's technology [3]. Current technology seems to be mature enough to allow spectrum sharing and coexistence among multiple systems. This, of course, requires more *tolerance* and *altruism* for a side-by-side coexistence. On the other hand, strict spectrum policies are required to resolve possible conflicts of interest among systems.

1.2 Dynamic Spectrum Access and Cognitive Radios

The inefficiency of current static spectrum utilization is reminiscent of the inefficiency of static TDMA for bursty traffic, or in general, the inefficiency of static versus dynamic techniques. A variety of ideas have been proposed to bring about the required spectrum reform and improve the efficiency of its usage, which are all categorized under the general term *Dynamic Spectrum Access* (DSA) [4].

In this dissertation, we consider a hierarchical model. This model consists of two classes of spectrum users called primary and secondary. The first class, the primary users, are the more favored ones since they possess the license, and therefore the right to use the spectrum without any restriction and when and where they need it. On the other hand, the spectrum is open for the use of secondary unlicensed users, as long as their interference perceived by a primary user is less than some threshold. That is required so that their presence goes unnoticed for the primary users.

This responsibility to be vigilant and have an open eye on their operation to limit their interference to the primary users, requires that secondary nodes to be more intelligent and cognitive compared to the conventional wireless devices. In parallel to this recognition, new ideas have been proposed for an intelligent device called *Cognitive Radio* (CR)[5]. The idea is that CRs have the capability of learning from their surrounding environment and adapting to the statistical variations of the input stimuli. In other words, these radios basically mimic the learning process of human brain.

The concept of CR is an extension of the original idea of *Software Defined Radio* (SDR) [6]. A basic definition of SDR is: a radio in which some or all of the physical layer functions

are software defined [7]. CRs can be considered SDRs equipped with artificial intelligence, which make them capable of sensing and reacting to their environment.

Various methods have been proposed to employ this cognition capability and make the coexistence possible, which seek to *underlay*, *overlay* or *interweave* the secondary users' signals with those of the primary users [8]. In the underlay approach, concurrent primary and secondary transmissions are allowed, while power constraints are imposed on the secondary users so that their aggregate interference is below the noise floor of primary users [9]. An example is UWB system where signals with very high bandwidth and very low power spectral density are used. The low power spectral density tends to minimize the interference to primary users.

In the overlay scenario, the secondary nodes can decode the primary message and use techniques like dirty paper coding [10] or employ cooperative methods to cancel interference at both primary and secondary nodes. Reference [11] considers a two-sender two-receiver interference channel model, in which sender 2 obtains the encoded message from user 1 in a causal or noncausal manner. Achievable rate regions are found by using ideas from Gel'fand and Pinsker's coding scheme [12]. Reference [13] discusses that cooperation between secondary nodes for transmission of their own data or cooperative transmission of primary traffic (cognitive relaying) can greatly benefit the implementation of cognitive radio.

In the interweave approach, secondary nodes try to detect void space-time-frequency holes and exploit them for their own transmission. *Opportunistic Spectrum Access* (OSA) is an alternative name used for this method. In [14], a two-switch model is developed that captures the spectral activity estimates at the cognitive transmitter and receiver. Upper and lower bounds are obtained for the capacity of the cognitive radio channel.

1.3 Interference: The Achilles' Heel

In this dissertation, we are mostly concerned with the underlay approach. On the premise that they do not harmfully interfere with their primary counterparts, secondary nodes

are allowed to operate concurrently with the primary. Interference can be considered as the point of vulnerability in the cognitive wireless networks and interference avoidance is, therefore, the most important step toward the implementation of such networks.

In [15], a resource allocation framework is presented for spectrum underlay in cognitive radio networks. Joint admission and power control algorithms are proposed to satisfy both the interference constraint for primary users and Quality of Service (QoS) constraint (in terms of a minimum SINR) for secondary users.

Reference [16] develops an analytical framework for opportunistic spectrum access based on the theory of Partially Observable Markov Decision Processes (POMDP). Under this framework, cognitive MAC protocols are proposed that optimize the performance of secondary users while limiting the interference perceived by primary users.

In [17], a spectrum sharing problem is considered in an unlicensed band where multiple systems coexist and interfere with each other. The authors use a repeated game framework to model the interaction of the coexisting systems assuming that they work for a long period of time. The outcome of this repeated game is shown to be self-enforcing, efficient and fair.

Reference [18] studies the problem of joint power control and beamforming with the objective of minimizing the total transmit power of the cognitive network, such that the received interference at the primary users remain below a threshold level and a minimum SINR is guaranteed at the secondary users who are admitted in the system.

To minimize the interference from secondary network to primary nodes, power control strategies have been proposed for secondary nodes. In [19], considering an interference temperature constraint and assuming that channel gains are common knowledge among the secondary nodes, the optimal power control is modeled as a concave minimization problem and an improved branch and bound algorithm is used to address it. Reference [20] proposes transmit power control using a fuzzy logic system to address the coexistence problem. The distances between secondary nodes and a primary node is estimated based on empirical propagation formulas for the path loss. In [21], the power control problem for a cognitive radio ad hoc network, coexisting with the legacy TV system, is formulated and centralized

and distributed algorithms are derived. In [22], a noncooperative power control model is proposed for the secondary network using game theory and exponential pricing.

1.4 Interference Modeling

To achieve the coexistence goal, interference modeling is of great significance. Interference, in general, has a stochastic nature not only due to randomness in the propagation channel, but also due to the random geographic dispersion of nodes. A statistical representation for interference, in which the power levels of the secondary nodes influence the parameters of the model, is, thus, of considerable interest in analysis and design of cognitive wireless network.

There are few prior work for characterizing interference in cognitive radio networks. Reference [23] considers a victim receiver subject to a Poisson field of Continuous Wave (CW) interferers¹, in an unlicensed band. The authors discuss the impact of the density of interferers on the average Bit Error Rate (BER).

In [25], a model is proposed for cognitive wireless networks which is based on spatial bivariate Poisson processes. Assuming a simple Gaussian model for interference, power control strategies are devised for secondary network to avoid interference on the primary nodes.

Reference [26] considers the characterization of the aggregated interference, ignoring how individual nodes can contribute in the total interference, i.e., no indexing is considered among the secondary nodes. The author finds closed-form expressions for the cumulants of aggregated interference and proposes that the interference can be approximated using a Shifted Log-normal (SLN) random variable.

In [27], the authors propose a model for aggregate interference based on the sum of a Normal and Log-normal random variables in which the parameters of the model are influenced by the power levels in the secondary network. Power control strategies are proposed for interference avoidance on the primary node.

¹The authors in [23] borrow the notion of *Poisson field of interferers* from [24].

1.4.1 Modeling of Cognitive Wireless Networks

An integral part to developing a realistic model of interference in cognitive wireless networks, is to have a model for the coexisting primary and secondary networks.

Most of the models considered in the literature so far, are based on some simplifying assumptions. Primary and secondary nodes are considered to be deterministic finite networks in which nodes have perfect knowledge of secondary-secondary and secondary-primary path gains. Usually a single primary Base Station (BS) is considered and the goal is to optimize some objective function in the secondary network (e.g., maximizing throughput or minimizing transmit power) while ensuring that the interference to the primary BS is less than some threshold.

The location of nodes in a network, due to factors like mobility, unplanned placement of the nodes (e.g., in mesh and sensor networks), etc, may be considered as realizations of spatial point processes. In this dissertation, we consider primary and secondary networks as two intertwined random wireless networks.

Except in some special cases, these processes are often difficult to deal with and closed-form solutions are hard to find [28]. The Poisson point process has been an attractive candidate for modeling these random structures as it often leads to closed-form solutions [29].

1.4.2 Stochastic Geometry for Modeling the Coexisting Networks

In reference [30], considering a spatial Poisson model for a random wireless network, the internodal distances are found to have a generalized Gamma distribution. Consequently, considering a finite version of the above model (i.e., using spatial Binomial processes), the distribution of internodal distances are shown to have a generalized Beta distribution in [31].

In [25] and [32], using a spatial bivariate Poisson model, the results found in [30] are extended to consider the case that each node belongs to one of the two distinguishable types (e.g., in networks with heterogeneous node types), and the number of nodes of each

type in a given region are marginally Poisson distributed and correlated. The distribution of distances between pairs of nodes of dissimilar types and some useful statistics of these distances are found. An immediate application of the spatial bivariate Poisson process is in modeling the heterogeneous two-type wireless networks. One typical example is the cognitive wireless networks.

1.5 Outline and Contribution of Dissertation

The remainder of this dissertation is organized as follows. Chapter 2, considers the distances in spatial bivariate Poisson point processes. The chapter is based, in part, on the results obtained in [25], [32] and [33]. This model will be later used to characterize the coexisting wireless networks, and the results obtained will be used to characterize the interference from secondary network to primary nodes and from secondary nodes to a given secondary node.

In Chapter 3, by using the analytical results obtained in Chapter 2, the interference from secondary neighbors of a primary node to the primary node is characterized. Two different models are developed for modeling the interference. In each model, the parameters are shown to be adjustable by changing the power levels in the secondary network. Furthermore, the interference constraint and the models' parameters are modified in case a statistical model is considered for secondary transmission and primary reception.

In Chapter 4, considering the interference models developed in Chapter 3, power control strategies are devised to satisfy the interference constraint. Chapters 3 and 4 are based on the results obtained in [25] and [27].

In Chapter 5, analytical results are obtained for the lower bound of achievable throughput in the power-constrained secondary network. We consider different forwarding strategies (nearest neighbor forwarding and forwarding based on a probability distribution) and compare the achievable throughput in each case. The analytical results obtained in Chapter 2 for the real moments of distances are used in the derivations. This chapter is based on the results found in [33].

In Chapter 6, a summary of the contributions of this dissertation is presented and some

remarks are made for possible future research.

Chapter 2: Distances in Spatial Point Processes

Points are the basic constituents in geometry. In the context of stochastic geometry, point processes (or *point patterns* in statistical terminology) are of interest. These processes are suitable mathematical tools for modeling data in a variety of scientific disciplines: ecology, seismology, spatial epidemiology, etc. Stochastic geometry has also been used in modeling the architecture of communication networks [34]. In this chapter, first, we explain two spatial point processes with applications in modeling random networks, i.e., *Poisson* and *Binomial* processes. We discuss the distances in these processes in which points are of non-distinguishable type. We extend the results for the case of spatial *bivariate* or *two-type* Poisson processes and derive some statistical properties of distances in these processes. These properties will be used in the following chapters for interference modeling, devising power control strategies for interference avoidance, and obtaining theoretical limits for the achievable throughput in cognitive wireless networks.

2.1 Spatial Point Processes With Single-Type Points

Most of the existing work on spatial point processes are for processes in which points are of a single type. The implication of this property is that they can be used only for modeling networks with nodes of homogeneous type. In this section we describe two point processes which have found applications in modeling random homogeneous networks.

2.1.1 Spatial Poisson Point Processes

Consider a homogeneous m -dimensional Poisson process with intensity λ and assume that $A \subset \mathcal{R}^m$ is a bounded Borel set ¹. Then, the probability that k points exist in A is

$$\Pr\{k \text{ points exist in } A\} = e^{-\lambda\nu(A)} \frac{(\lambda\Omega(A))^k}{k!}, \quad k = 0, 1, \dots \quad (2.1)$$

where $\Omega(A)$ is the Lebesgue measure of A ². For $A \cap B = \emptyset$, the number of points in A and B are *independent*. This property makes the Poisson process suitable for modeling uniformly random networks. In Figure 2-1, we have plotted a sample two-dimensional spatial Poisson point process with intensity $\lambda = 1$.

The distances between an arbitrary point and its neighboring points are of particular mathematical and practical interest. Following theorem is due to Haengi [30]:

Theorem 2.1. For a Poisson point process in \mathcal{R}^m with intensity λ , the Euclidean distance between a point and its n th nearest neighbor, R_n , is distributed according to the *generalized Gamma* distribution:

$$f_{R_n}(r) = e^{-\lambda c_m r^m} \frac{m(\lambda c_m r^m)^n}{r\Gamma(n)}, \quad r > 0, \quad (2.2)$$

where $c_m r^m$ is the volume of the m -dimensional ball of radius r and c_m is given by

$$c_m = \begin{cases} \frac{\pi^{m/2}}{(\frac{m}{2})!}, & \text{even } m \\ \frac{\pi^{\frac{m-1}{2}} 2^m (\frac{m-1}{2})}{m!} & \text{odd } m \end{cases} \quad (2.3)$$

¹Roughly speaking, Borel sets are the sets that can be constructed from open or closed sets by repeatedly taking countable unions and intersections. For more rigorous definition see [28].

²The Lebesgue measure can be considered an extension of the classical notions of length and area to higher dimensional sets [28].

and $\Gamma(n)$ is the gamma function,

$$\Gamma(z) = \int_0^\infty t^{z-1} e^{-t} dt, \quad (2.4)$$

evaluated at³ n .

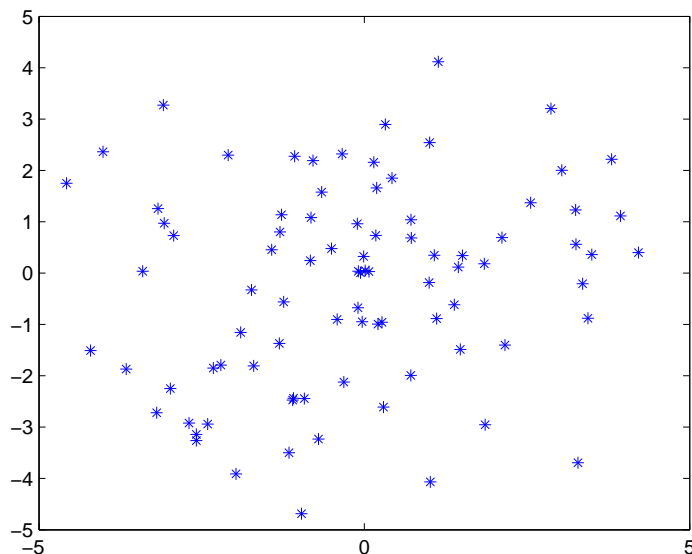


Figure 2.1: A sample 2-D spatial Poisson process with intensity $\lambda = 1$ where points are distributed in a disc of radius 5.

2.1.2 Spatial Binomial Point Processes

Consider an m -dimensional Binomial point process where N points are distributed in the Borel set $A \subset \mathcal{R}^m$. For any Borel subset B of A , the probability that k points exist in B is

$$\Pr\{k \text{ points exist in } B\} = \binom{N}{k} p^k (1-p)^{N-k} \quad (2.5)$$

³Note that for n , a positive integer, $\Gamma(n) = (n-1)!$

where $p = \frac{\Omega(B)}{\Omega(A)}$. In a similar fashion, number of points in more than two disjoint sets are related through a *multinomial* distribution. Following theorem is due to [31]:

Theorem 2.2. In a Binomial point process with N points distributed in a m -dimensional ball of radius R centered at the origin, the Euclidean distance between origin and its n th nearest point R_n , is distributed as a *generalized Beta* distribution:

$$f_{R_n}(r) = \frac{m}{R} \frac{B(n+1-1/m, N-n+1)}{B(N-n+1, n)} \beta\left(\left(\frac{r}{R}\right)^m; n+1-\frac{1}{m}, N-n+1\right), \quad r \in [0, R], \quad (2.6)$$

where $\beta(x; a, b) = \frac{1}{B(a, b)} x^{a-1} (1-x)^{b-1}$ is the beta density function and $B(a, b) = \frac{\Gamma(a)\Gamma(b)}{\Gamma(a+b)}$.

Reference [31], considers the above model for a system with N nodes distributed randomly and the BS at origin, and discusses applications of this result in issues like energy efficiency, localization, connectivity and computing the outage probability.

2.2 Spatial Bivariate Poisson Processes

We consider a spatial point process, in which, each point is tagged with one of the two possible labels. These processes are called bivariate or two-type spatial point processes [35]. The points of each type is marginally distributed according to a specific spatial Poisson point process. We distinguish between these points as type-A and type-B.

A general model in which the number of type-A and type-B points in an area are correlated is considered. So, points of each type having marginal Poisson distribution, also have some sort of association. This association can be formally represented by considering a spatial bivariate Poisson point process.

Unlike bivariate Poisson processes defined on the real line, there have been little work on the definition of spatial bivariate Poisson distribution (e.g., [35], [36]). In this chapter, we use an approach similar to [36] for the construction of these processes.

We consider three possible events: A, B, and AB (implying joint occurrence of both types), with the intensities λ , μ and ν , respectively. Unlike the one-dimensional bivariate Poisson case, in which joint occurrence implies the two events occur at exactly the same time instant, the occurrence of both types A and B at the same spatial point is not meaningful from a practical perspective as it implies the existence of two different objects at exactly the same location. To overcome this problem, a reference spatial Poisson process with intensity $\lambda + \mu + \nu$ is defined in [36]. Given that an event of this process has occurred at the spatial point \mathbf{y} , with probability $\frac{\lambda}{\lambda + \mu + \nu}$, there is a point of type A at \mathbf{y} , with probability $\frac{\mu}{\lambda + \mu + \nu}$, the point at \mathbf{y} is of type B and with probability $\frac{\nu}{\lambda + \mu + \nu}$ there is a type-A point at \mathbf{x}_1 and a type-B point at \mathbf{x}_2 . The locations of \mathbf{x}_1 and \mathbf{x}_2 are such that $\|\mathbf{x}_1 - \mathbf{y}\|$ and $\|\mathbf{x}_2 - \mathbf{y}\|$ ⁴ are independent random variables with probability density functions respectively $f(\|\mathbf{x}_1 - \mathbf{y}\|)$ and $g(\|\mathbf{x}_2 - \mathbf{y}\|)$.

We classify a point as either single (corresponding to events A or B) or double (i.e., being double with a point of the other type, corresponding to event AB). Then, we have the following probabilities:

$$\Pr\{\text{a single type-A point at } d\mathbf{x}_1\} = \lambda d\mathbf{x}_1,$$

$$\Pr\{\text{a single type-B point at } d\mathbf{x}_2\} = \mu d\mathbf{x}_2.$$

where $d\mathbf{x}_1$ and $d\mathbf{x}_2$ are respectively infinitesimally small areas at points \mathbf{x}_1 and \mathbf{x}_2 .

To find probability of double points, we need to consider all possible \mathbf{y} 's of the reference

⁴The distance metric is Euclidean.

Poisson process.

$$\begin{aligned}
& \Pr\{\text{a double point with A at } d\mathbf{x}_1 \text{ and B at } d\mathbf{x}_2\} \\
&= \nu \int_{\mathbf{y}} f(\|\mathbf{x}_1 - \mathbf{y}\|)g(\|\mathbf{x}_2 - \mathbf{y}\|)d\mathbf{y} \\
&= \nu h(\mathbf{x}_1, \mathbf{x}_2)d\mathbf{x}_1 d\mathbf{x}_2,
\end{aligned} \tag{2.7}$$

where $h(\mathbf{x}_1, \mathbf{x}_2)$ is defined as

$$h(\mathbf{x}_1, \mathbf{x}_2) \triangleq \int_{\mathbf{y}} f(\|\mathbf{x}_1 - \mathbf{y}\|)g(\|\mathbf{x}_2 - \mathbf{y}\|)d\mathbf{y}. \tag{2.8}$$

Note that integration of $h(\mathbf{x}_1, \mathbf{x}_2)$ on either \mathbf{x}_1 or \mathbf{x}_2 equals 1. So we have:

$$\begin{aligned}
\Pr\{\text{a double point at } d\mathbf{x}_1\} &= \nu \int_{\mathbf{x}_2} h(\mathbf{x}_1, \mathbf{x}_2)d\mathbf{x}_1 d\mathbf{x}_2 \\
&= \nu \int_{\mathbf{x}_2} h(\mathbf{x}_2, \mathbf{x}_1)d\mathbf{x}_1 d\mathbf{x}_2 \\
&= \nu d\mathbf{x}_1.
\end{aligned}$$

Using the above equation, we have

$$\begin{aligned}
\Pr\{\text{a type-A point at } d\mathbf{x}_1\} &= \lambda d\mathbf{x}_1 + \nu d\mathbf{x}_1 \\
&= (\lambda + \nu)d\mathbf{x}_1.
\end{aligned}$$

Similarly,

$$\Pr\{\text{a type-B point at } d\mathbf{x}_2\} = (\mu + \nu)d\mathbf{x}_2.$$

So, the number of type-A and type-B points in the two-dimensional region \mathcal{R} with area S

are each marginally Poisson distributed with parameters respectively $(\lambda + \nu)S$ and $(\mu + \nu)S$. The covariance of number of type-A points $N(A)$ and type-B points $N(B)$ in \mathcal{R} is given in [36] as

$$\text{Cov}\{N(A), N(B)\} = \nu \int_{\mathbf{x}_1, \mathbf{x}_2 \in \mathcal{R}} h(\mathbf{x}_1, \mathbf{x}_2) d\mathbf{x}_1 d\mathbf{x}_2. \quad (2.9)$$

2.2.1 Distance to n th Nearest Neighbor Distribution

In this subsection we seek to find the pdf of the distance from a point of one particular type to its n th nearest neighbor of the other type. In the absence of correlation between the two types, the existence of a point does not have any influence on the points of the other type. On the other hand, if the two types are correlated, each point has an impact on the distribution of the other type points. The distance of a point to its n th neighbor (of the same type) was shown in the previous section to have generalized Gamma distribution (see Theorem 1). The question still remains: what is the distribution of the distance of a type A (B) point to its n th nearest neighbor of type B (A)? Let us denote these distances as $R_{AB,n}$ and $R_{BA,n}$ respectively (see Figure 2-2). Define the following events:

$$\mathcal{E}_1 = \{\text{There is a type-A point at } d\mathbf{x}_1\}$$

and

$$\mathcal{E}_2 = \{\text{There is a type-B point at } d\mathbf{x}_2\}.$$

A type-A point at $d\mathbf{x}_1$ and a type-B point at $d\mathbf{x}_2$ can be:

- single points with probability $\lambda d\mathbf{x}_1 \mu d\mathbf{x}_2$,
- together as double points with probability $\nu h(\mathbf{x}_1, \mathbf{x}_2) d\mathbf{x}_1 d\mathbf{x}_2$,
- A single but B double with probability $\lambda d\mathbf{x}_1 \nu d\mathbf{x}_2$,
- A double but B single with probability $\nu d\mathbf{x}_1 \mu d\mathbf{x}_2$.

Then we have:

$$\begin{aligned}
\Pr\{\mathcal{E}_2|\mathcal{E}_1\} &= \frac{\Pr\{\mathcal{E}_1 \cap \mathcal{E}_2\}}{\Pr\{\mathcal{E}_1\}} \\
&= \frac{\lambda d\mathbf{x}_1 \mu d\mathbf{x}_2 + \nu h(\mathbf{x}_1, \mathbf{x}_2) d\mathbf{x}_1 d\mathbf{x}_2 + \lambda d\mathbf{x}_1 \nu d\mathbf{x}_2 + \nu d\mathbf{x}_1 \mu d\mathbf{x}_2}{(\lambda + \nu) d\mathbf{x}_1} \\
&= \left[\mu + \frac{\nu}{\lambda + \nu} (\lambda + h(\mathbf{x}_1, \mathbf{x}_2)) \right] d\mathbf{x}_2.
\end{aligned} \tag{2.10}$$

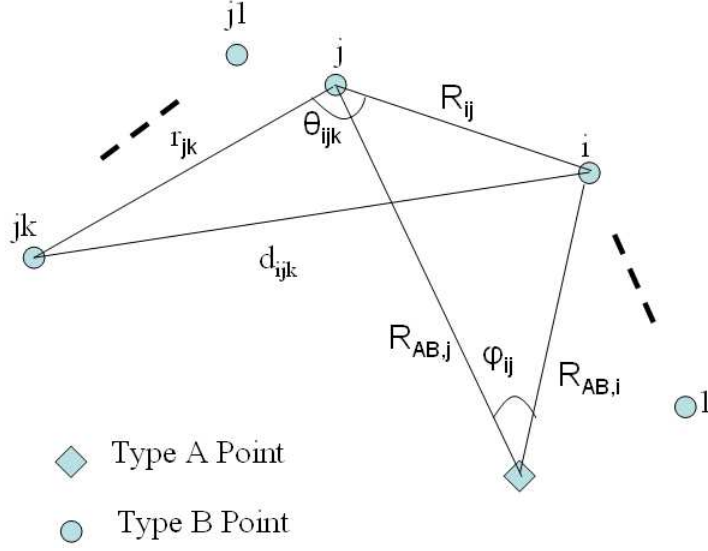


Figure 2.2: node i is the i th nearest type-B neighbor of a type-A point. node jk is the k th nearest type-B neighbor of node j .

From (2.10), we see that given a type-A point exists at $d\mathbf{x}_1$, the intensity of type-B points is nonhomogeneous due to the $h(\mathbf{x}_1, \mathbf{x}_2)$ term. In other words, the conditional intensity of a type-B point at \mathbf{x}_2 will be

$$\Lambda(\mathbf{x}_2) = \mu + \frac{\nu}{\lambda + \nu} (\lambda + h(\mathbf{x}_1, \mathbf{x}_2)). \tag{2.11}$$

The expected number of type-B events in an area would then be the integral of the above intensity function in that area. For example, let us denote the ring with the type-A point

as center and inner and outer radii of respectively r_0 and r ($r_0 \ll r$) as \mathcal{C} . The expected number of type-B points in \mathcal{C} is

$$\chi(r) = \int_{\mathbf{x}_2 \in \mathcal{C}} \Lambda(\mathbf{x}_2) d\mathbf{x}_2. \quad (2.12)$$

Lemma 1. The pdf of the distance to the n th type-B neighbor of a type-A point is

$$f_{R_{AB,n}}(r) = e^{-\chi(r)} \frac{d\chi(r)}{dr} \frac{\chi(r)^{n-1}}{(n-1)!}. \quad (2.13)$$

Proof. The Complementary Cumulative Distribution Function (CCDF) of $R_{AB,n}$ can be calculated as

$$\begin{aligned} F_{c,R_{AB,n}}(r) &= \Pr\{R_{AB,n} > r\} \\ &= \Pr\{\text{There are less than } n \text{ type-B points in } \mathcal{C}\} \\ &= \sum_{k=0}^{n-1} e^{-\chi(r)} \frac{\chi(r)^k}{k!}. \end{aligned} \quad (2.14)$$

The pdf of $R_{AB,n}$ can be found as

$$\begin{aligned} f_{R_{AB,n}}(r) &= -\frac{dF_{c,R_{AB,n}}(r)}{dr} \\ &= e^{-\chi(r)} \frac{d\chi(r)}{dr} \left[\sum_{k=0}^{n-1} \frac{\chi(r)^k}{k!} - \sum_{k=1}^{n-1} \frac{\chi(r)^{k-1}}{(k-1)!} \right] \\ &= e^{-\chi(r)} \frac{d\chi(r)}{dr} \frac{\chi(r)^{n-1}}{(n-1)!}. \end{aligned} \quad \square$$

Corollary 1. The expected value of the distance to the n th type-B neighbor is

$$E\{R_{AB,n}\} = \int_0^\infty F_{c,R_{AB,n}}(r) dr = \sum_{k=0}^{n-1} \int_0^\infty e^{-\chi(r)} \frac{\chi(r)^k}{k!} dr \quad (2.15)$$

In particular, defining $r_{AB} \triangleq R_{AB,1}$ as the distance of a type-A point from its nearest neighbor of type B, we have

$$E\{r_{AB}\} = \int_0^\infty e^{-\chi(r)} dr \quad (2.16)$$

and from (2.13)

$$f_{r_{AB}}(r) = e^{-\chi(r)} \frac{d\chi(r)}{dr}. \quad (2.17)$$

From (2.9), we see that the choice of ν and $h(\mathbf{x}_1, \mathbf{x}_2)$ influences the correlation between number of type-A and type-B points. In [36], $h(\mathbf{x}_1, \mathbf{x}_2)$ is calculated when $f(\mathbf{x})$ and $g(\mathbf{x})$ are zero-mean isotropic Gaussian distributions with variances σ_1^2 and σ_2^2 , respectively:

$$h(\mathbf{x}_1, \mathbf{x}_2) = h(\mathbf{x}_1 - \mathbf{x}_2, \mathbf{0}) = h(\mathbf{x}, \mathbf{0}) = \frac{1}{2\pi\sigma^2} e^{-\frac{\|\mathbf{x}\|^2}{2\sigma^2}}, \quad (2.18)$$

where $\mathbf{x} = \mathbf{x}_1 - \mathbf{x}_2$ and $\sigma^2 = \sigma_1^2 + \sigma_2^2$.

The parameter σ impacts on the correlation between primary and secondary nodes. Given a primary node exists at origin, and for a fixed region of integration and a fixed value of ν , a high value of σ implies a narrow Gaussian function and therefore a high correlation (see (2.9) and (2.18)) and vice versa. In Figure 2-3, using (2.11) and (2.18), the conditional intensity of type-B points at point \mathbf{x} , given a type-A point exists at the origin is shown for different values of ν and for the given parameters. When $\nu = 0$, due to the lack of correlation between type-A and type-B points, we can see that the existence of the type-A point at origin does not have any influence on type-B points as their intensity will remain

fixed (i.e., $\mu = 2$). As ν increases, there will be a higher chance that type-B points exist near the origin.

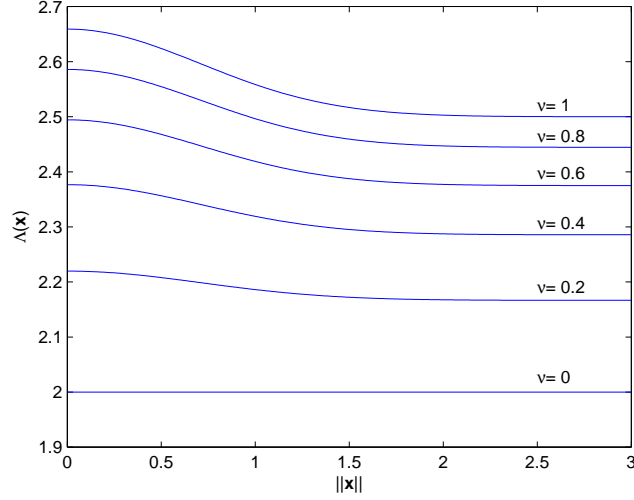


Figure 2.3: Conditional intensity of type-B points given a type-A point exists at the origin ($\lambda = 1$, $\mu = 2$, and $\sigma^2 = 0.5$).

For the $h(\mathbf{x}_1, \mathbf{x}_2)$ in (2.18), $\chi(r)$ can be found using (2.12) as

$$\chi(r) = \left(\mu + \frac{\nu\lambda}{\nu + \lambda}\right)\pi(r^2 - r_0^2) + \frac{\nu}{\nu + \lambda}\left(e^{\frac{-r_0^2}{2\sigma^2}} - e^{\frac{-r^2}{2\sigma^2}}\right). \quad (2.19)$$

In Figure 2-4, we have sketched the pdf of r_{AB} , the distance of the type-A point to its nearest type-B neighbor, for various values of ν and assuming $r_0 = 0$. For $\nu = 0$ the pdf is that of generalized Gamma distribution (see Theorem 1). As ν increases the distribution is tilted toward left, which means, with a higher probability, the nearest neighbor is located in a closer distance to the type-A point.

In Figure 2-4, $E\{r_{AB}\}$ is plotted versus ν and as expected its value decreases as ν increases.

We can rewrite equation (2.19) as

$$\chi(r) = a(r^2 - r_0^2) + b(e^{-cr_0^2} - e^{-cr^2}),$$

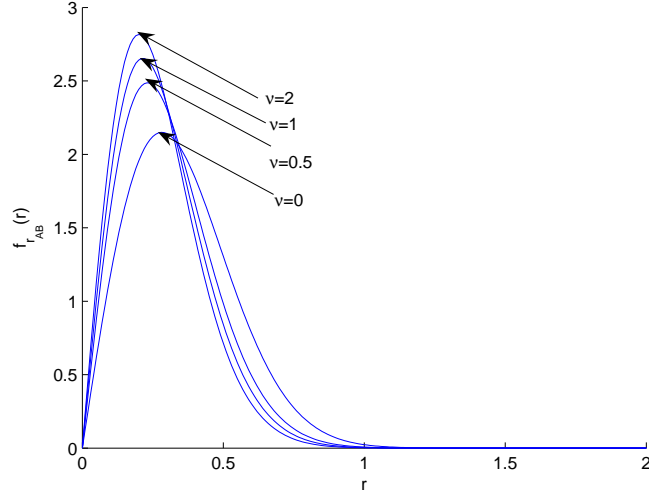


Figure 2.4: $f_{r_{AB}}(r)$ ($\lambda = 1$, $\mu = 2$, and $\sigma^2 = 0.1$).

with $a = (\mu + \frac{\nu\lambda}{\nu+\lambda})\pi$, $b = \frac{\nu}{\lambda+\nu}$, and $c = \frac{1}{2\sigma^2}$. For $\sigma \gg 1$, $e^{-cr^2} \approx 1 - cr^2$, and we have

$$\chi(r) \approx (a + bc)(r^2 - r_0^2) \approx (a + bc)r^2. \quad (2.20)$$

where the second approximation is based on the assumption $r_0 \ll r$.

Lemma 2. The expected value of $R_{PS,n}^\alpha$, for α a real number and $\sigma^2 \gg 1$, is

$$E\{R_{PS,n}^\alpha\} = \frac{\Gamma(n + \alpha/2)}{(a + bc)^{\alpha/2}(n-1)!}, \quad n \geq -[\alpha/2]. \quad (2.21)$$

where $[x]$ is, by definition, the largest integer, smaller than or equal to x . For $n < -[\alpha/2]$, defining $f_n(x) = x^{n+\alpha/2-1}$, and for M large enough, we have

$$E\{R_{PS,n}^\alpha\} \approx \frac{1}{(a + bc)^{\alpha/2}(n-1)!} \sum_{i=1}^M w_i f_n(x_i), \quad n < -[\alpha/2], \quad (2.22)$$

where x_i and w_i are the abscissas and the weights for Gauss-Laguerre quadrature of order M .

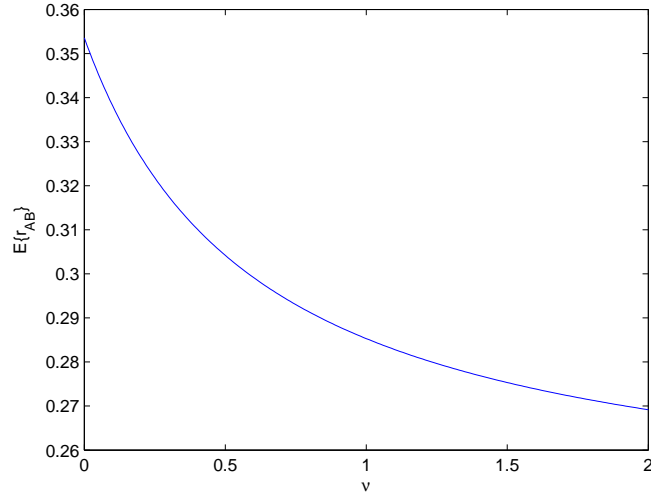


Figure 2.5: $E\{r_{AB}\}$ ($\lambda = 1$, $\mu = 2$, and $\sigma^2 = 0.1$).

Proof. Expected value of $R_{PS,n}^\alpha$ is found as

$$E\{R_{PS,n}^\alpha\} = \int_0^\infty r^\alpha f_{R_{PS,n}(r)} dr = \int_0^\infty r^\alpha e^{-\chi(r)} \frac{\chi(r)^{n-1}}{(n-1)!} d\chi(r).$$

Using integration by substitution with $u = \chi(r)$ and $r = \chi^{-1}(u) = g(u)$, we will have

$$E\{R_{PS,n}^\alpha\} = \int_0^\infty g^\alpha(u) \frac{u^{n-1}}{(n-1)!} e^{-u} du.$$

When $\sigma^2 \gg 1$, $\chi(r) \approx (a+bc)r^2$, $g(u) \simeq \sqrt{\frac{u}{a+bc}}$ and we have

$$E\{R_{PS,n}^\alpha\} = \frac{1}{(a+bc)^{\alpha/2}(n-1)!} \int_0^\infty u^{n+\alpha/2-1} e^{-u} du. \quad (2.23)$$

Using (2.23) and noting that

$$\int_0^\infty x^q e^{-x} dx = \Gamma(q+1), \quad q > -1$$

we will get the result in (2.21). The integral in (2.23) does not have closed form solution for $n < -[\alpha/2]$. In this case, with $f_n(x) = x^{n+\alpha/2-1}$, we use the Gauss-Laguerre quadrature rule

$$\int_0^\infty e^{-x} f_n(x) dx = \sum_{i=1}^M w_i f_n(x_i) + R_M. \quad (2.24)$$

Here, M is the number of sample points used for integration. The larger the value of M , the closer the approximation:

$$\int_0^\infty e^{-x} f_n(x) dx \approx \sum_{i=1}^M w_i f_n(x_i). \quad (2.25)$$

The abscissa x_i is the i th root of Laguerre polynomial $L_M(x)$ [37] ($i = 1, 2, \dots, M$), and the weights are

$$w_i = \frac{(M!)^2 x_i}{(M+1)^2 [L_{M+1}(x_i)]^2}. \quad (2.26)$$

x_i and w_i for different values of M are tabulated in [37]. □

This is a general result and can be applied in case of primary and secondary nodes being independently distributed as well, in which case we will have $\nu = 0$, $b = 0$, and $a = \mu\pi$.

It can be seen from (2.20) that conditioned on a single primary node, the secondary nodes are distributed according to a homogeneous Poisson process with conditional intensity of $(a+bc)/\pi$. Defining $\lambda_c \triangleq a+bc$, in following lemma, we show that $Z_n = R_{AB,n}^2$ is distributed according to an Erlang distribution with mean n/λ_c .

Lemma 3. :Defining $Z_n \triangleq R_{AB,n}^2$, Z_n has an Erlang distribution with mean n/λ_c .

Proof. For $Z_n \triangleq R_{AB,n}^2$, the pdf of Z_n can be found using the transformation formula as

$$f_{Z_n}(z) = \frac{1}{2\sqrt{z}} f_{R_{AB,n}}(\sqrt{z}), \quad z > 0, \quad (2.27)$$

The pdf of $R_{AB,n}$ is given in equation (2.13). Using that in (2.27), with $\chi(r) = \lambda_c r^2$, we find

$$f_{Z_n}(z) = \lambda_c e^{-\lambda_c z} \frac{(\lambda_c z)^{n-1}}{(n-1)!}, \quad z > 0, \quad (2.28)$$

which is the pdf of an Erlang distribution with mean n/λ_c . □

Interestingly, Z_n has the distribution of the distance to n th arrival in a Poisson process on *real line*.

2.2.2 Distance between type-B neighbors of a type-A point

In Figure 2-2, φ_{ij} is the difference between two uniform random variables in $[0, 2\pi]$. In the following lemma, we find the cdf and pdf of φ_{ij} .

Lemma 4. The cdf and pdf of φ_{ij} are respectively as follow:

$$F_{\varphi_{ij}}(\varphi) = \begin{cases} 0, & \varphi < 0 \\ \frac{\varphi}{\pi} - \frac{\varphi^2}{4\pi^2} & 0 \leq \varphi < 2\pi \\ 1, & \varphi \geq 2\pi \end{cases} \quad (2.29)$$

and

$$f_{\varphi_{ij}}(\varphi) = \begin{cases} \frac{2\pi - \varphi}{2\pi^2} & 0 \leq \varphi \leq 2\pi \\ 0, & \text{otherwise} \end{cases} \quad (2.30)$$

Proof. We have $\varphi_{ij} = |\varphi_j - \varphi_i|$ where φ_i and φ_j are the angles associated with the polar

coordinates of the i th and j th nearest type-B neighbors of the type-A point and are uniform random variables in $[0, 2\pi]$. So we can write

$$F_{\varphi_{ij}}(\varphi) = \Pr\{|\varphi_j - \varphi_i| \leq \varphi\} = \int_0^{2\pi} \Pr\{|\varphi_j - \varphi_i| \leq \varphi | \varphi_i = \alpha\} f_{\varphi_i}(\alpha) d\alpha \quad (2.31)$$

Assuming the independence of φ_i and φ_j ,

$$F_{\varphi_{ij}}(\varphi) = \frac{1}{2\pi} \int_0^{2\pi} \Pr\{|\varphi_j - \alpha| \leq \varphi\} d\alpha. \quad (2.32)$$

For a fixed $0 \leq \varphi \leq 2\pi$, it can be verified that

$$\Pr\{|\varphi_j - \alpha| \leq \varphi\} = \begin{cases} \frac{\varphi + \alpha}{2\pi^2} & 0 \leq \alpha < \varphi \\ \frac{\varphi}{\pi}, & \varphi \leq \alpha < 2\pi - \varphi \\ \frac{2\pi - \alpha + \varphi}{2\pi}, & 2\pi - \varphi \leq \alpha \leq 2\pi \end{cases} \quad (2.33)$$

using (2.33) in (2.32) and taking the derivative, the cdf and pdf will be found as given in (2.29) and (2.30). \square

Lemma 5. Defining

$$a \triangleq E\{R_{AB,i}\} \quad \text{and} \quad b \triangleq E\{R_{AB,j}\}, \quad (2.34)$$

we have,

$$E\{R_{ij}^\alpha\} \approx \int_{b-a}^{b+a} \frac{2r^{\alpha+1}}{\sqrt{(r^2 - (b-a)^2)((b+a)^2 - r^2)}} \left[\frac{2}{\pi} - \frac{1}{\pi^2} \arccos\left(\frac{a^2 + b^2 - r^2}{2ab}\right) \right] dr \quad (2.35)$$

Proof. We use the shorthand notation of R_i for $R_{AB,i}$ and define $\theta = \arccos\left(\frac{R_i^2 + R_j^2 - r^2}{2R_i R_j}\right)$.

It follows that

$$F_{R_{ij}|R_i,R_j}(r) = 2\Pr\{0 \leq \varphi_{ij} \leq \theta\} = \begin{cases} 0, & 0 < r \leq R_j - R_i \\ 2 \left(\frac{\theta}{\pi} - \frac{\theta^2}{4\pi^2} \right), & R_j - R_i < r \leq R_j + R_i \\ 1, & r > R_j + R_i \end{cases} \quad (2.36)$$

and

$$f_{R_{ij}|R_i,R_j}(r) = \frac{d F_{R_{ij}|R_i,R_j}(r)}{dr} = \begin{cases} \frac{d\theta}{dr} \left(\frac{2}{\pi} - \frac{\theta}{\pi^2} \right), & R_j - R_i < r \leq R_j + R_i \\ 0, & \text{otherwise.} \end{cases} \quad (2.37)$$

where $\frac{d\theta}{dr} = \frac{2r}{\sqrt{[r^2 - (R_j - R_i)^2][(R_j + R_i)^2 - r^2]}}$. Using the conditional pdf, we have

$$\begin{aligned} E\{R_{ij}^\alpha\} &= E\{E\{R_{ij}^\alpha|R_i, R_j\}\} \\ &= E\left\{ \int_{R_j - R_i}^{R_j + R_i} r^\alpha f_{R_{ij}|R_i,R_j}(r) dr \right\} \end{aligned}$$

Defining

$$G(R_i, R_j) \triangleq \int_{R_j - R_i}^{R_j + R_i} r^\alpha f_{R_{ij}|R_i,R_j}(r) dr \quad (2.38)$$

we have

$$E\{R_{ij}^\alpha\} = E\{G(R_i, R_j)\} \approx G(E\{R_i\}, E\{R_j\}). \quad (2.39)$$

where the approximation is due to interchanging the expectation and function evaluation. Using the definition of a and b , we find the result. Simulation results show that (2.39) is a close approximation (see Figure 2-9). \square

Lemma 6. Assume θ_{ijk} is a uniform random variable in $[0, \pi]$. Simulation results show

that this is a valid assumption (see Figure 2-7). Also, define

$$\begin{aligned} c &= |E\{R_{ij}\} - E\{r_{jk}\}|, \\ d &= E\{R_{ij}\} + E\{r_{jk}\}. \end{aligned} \quad (2.40)$$

We have,

$$E\{d_{ijk}^\alpha\} = \frac{2}{\pi} \int_c^d \frac{\delta^{\alpha+1}}{\sqrt{(\delta^2 - c^2)(d^2 - \delta^2)}} d\delta \quad (2.41)$$

Proof. Since θ_{ijk} is uniform in $[0, \pi]$, it follows that

$$F_{d_{ijk}|R_{ij}, r_{jk}}(\delta) = \begin{cases} 0, & \delta < |R_{ij} - r_{jk}| \\ \frac{1}{\pi} \arccos\left(\frac{R_{ij}^2 + r_{jk}^2 - \delta^2}{2R_{ij}r_{jk}}\right), & |R_{ij} - r_{jk}| \leq \delta \leq R_{ij} + r_{jk} \\ 1, & \delta > R_{ij} + r_{jk} \end{cases} \quad (2.42)$$

and

$$f_{d_{ijk}|R_{ij}, r_{jk}}(\delta) = \begin{cases} \frac{2\delta}{\pi} \frac{1}{\sqrt{[(R_{ij} + r_{jk})^2 - \delta^2][\delta^2 - (R_{ij} - r_{jk})^2]}}, & |R_{ij} - r_{jk}| \leq \delta \leq R_{ij} + r_{jk} \\ 0, & \text{otherwise} \end{cases} \quad (2.43)$$

So, we have

$$E\{d_{ijk}^\alpha\} = E\{E\{d_{ijk}^\alpha | R_{ij}, r_{jk}\}\} = E\left\{\int_{|R_{ij} - r_{jk}|}^{R_{ij} + r_{jk}} \delta^\alpha f_{d_{ijk}|R_{ij}, r_{jk}}(\delta) d\delta\right\} \quad (2.44)$$

Defining

$$H(R_{ij}, r_{jk}) = \int_{|R_{ij} - r_{jk}|}^{R_{ij} + r_{jk}} \delta^\alpha f_{d_{ijk}|R_{ij}, r_{jk}}(\delta) d\delta \quad (2.45)$$

we have

$$E\{d_{ijkj}^\alpha\} = E\{H(R_{ij}, r_{jk})\} \approx H(E\{R_{ij}\}, E\{r_{jk}\}) \quad (2.46)$$

Using the definition of c and d , we find the result. Simulation results show that (2.46) is a close approximation (see Figure 2-10). \square

Consider a bivariate spatial Poisson process with parameters $\lambda = 0.005$, $\mu = 0.001$, and $\nu = 0.0025$ and a disc with radius $R = 1000$ units is considered as the underlying area in which points are present (i.e., $r_0 = 0$). Assume $\sigma^2 = 10$ to satisfy the condition $\sigma^2 \gg 1$. Given that a type-A point exists in the origin, the number of type-B points in the area, m , will be a Poisson random variable with mean $\bar{m} = \lambda_c R^2 = (a + bc)R^2 = 25044$.

To simulate a sample realization of this spatial bivariate Poisson process, each random type-B point at the polar coordinates (r, θ) is found using following formulas [28]

$$r = \sqrt{R^2 z_1} \quad (2.47)$$

$$\theta = 2\pi z_2, \quad (2.48)$$

where z_1 and z_2 are uniform random numbers in $[0, 1]$, and this is done for as many as m points.

In Figure 2-5, we have plotted the normalized histogram of φ_{ij} (for 10000 realization of the process) and the pdf obtained in (2.21) for $i = 10$ and $j = 20$. In Figure 2-6, the normalized histogram of θ_{ijk} along with uniform pdf is plotted. The result shows that the uniformity assumption is a reasonable assumption.

In Figure 2-7, we have obtained simulation results for the statistical mean of $R_{AB,n}^\alpha$ for different values of n (4 and 10). We have also plotted, alongside, the analytical results for $E\{R_{AB,n}^\alpha\}$. To obtain the statistical means, we have considered 2000 different realizations of the process and have averaged the results. The results show that analytical results follow

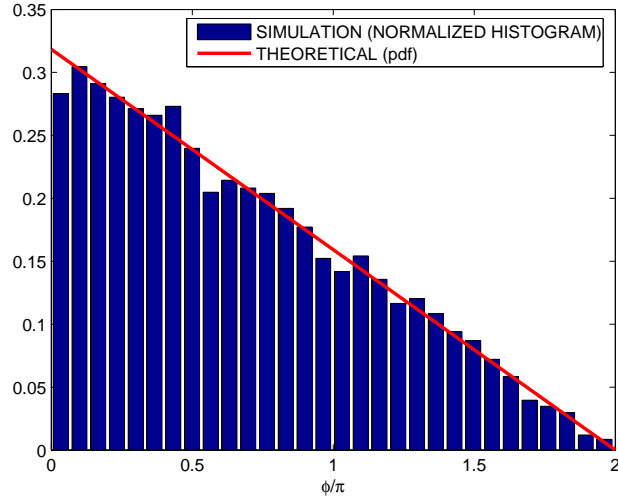


Figure 2.6: Normalized histogram and analytical pdf of φ_{ij} ($i = 10$ and $j = 20$).

the simulations very closely.

In Figure 2-8, simulation and analytical results for $E\{R_{ij}^\alpha\}$ (obtained in (2.26)) are plotted together, where we have assumed $i = 10$ and $j = 20$. We use one of the numerical integration methods available in MATLAB to find the definite integral in (2.26). The result shows that the assumption in (2.30) results in a good approximation.

In Figure 2-8, simulation and analytical results for $E\{d_{ijk}^\alpha\}$ (obtained in (2.32)) are plotted together, where we have assumed $i = 10$, $j = 20$ and $k = 5$. We again use numerical integration to find the definite integral in (2.32). The result shows that the assumption in (2.37) results in a good approximation.

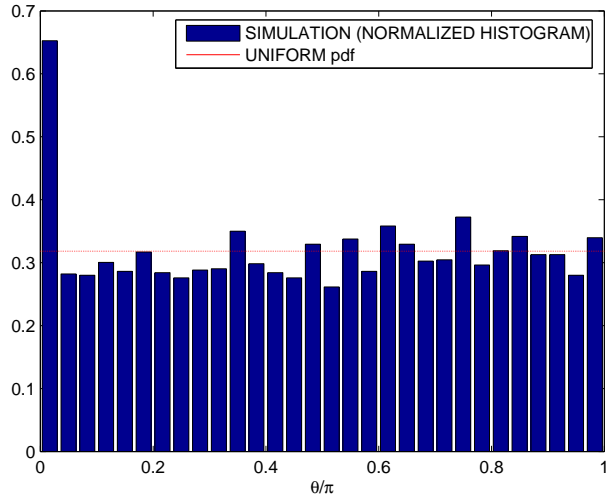


Figure 2.7: Normalized histogram of θ_{ijk} and uniform pdf ($i = 10$, $j = 20$ and $k = 5$).

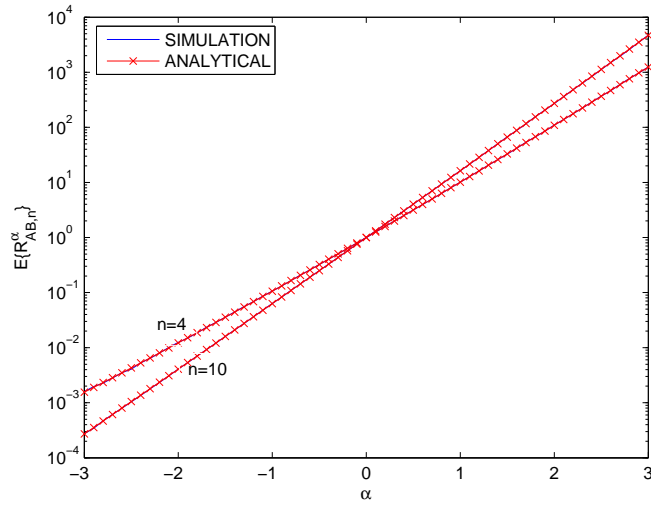


Figure 2.8: Simulation (statistical mean) and analytical result for $E\{R_{AB,n}^\alpha\}$

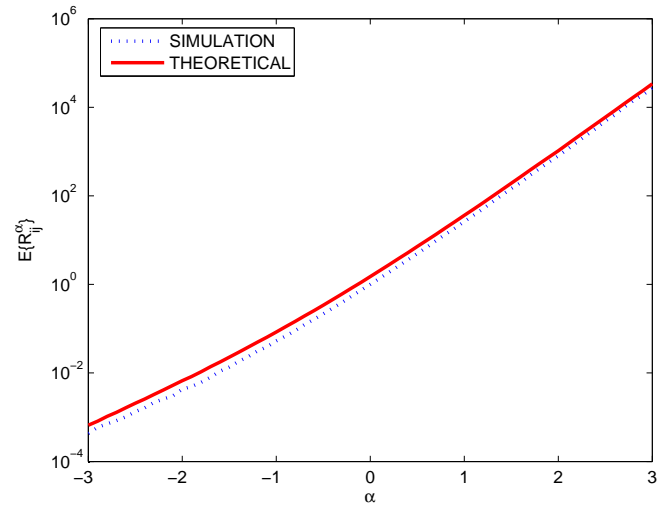


Figure 2.9: Simulation (statistical mean) and analytical result for $E\{R_{ij}^\alpha\}$ ($i = 10$ and $j = 20$)

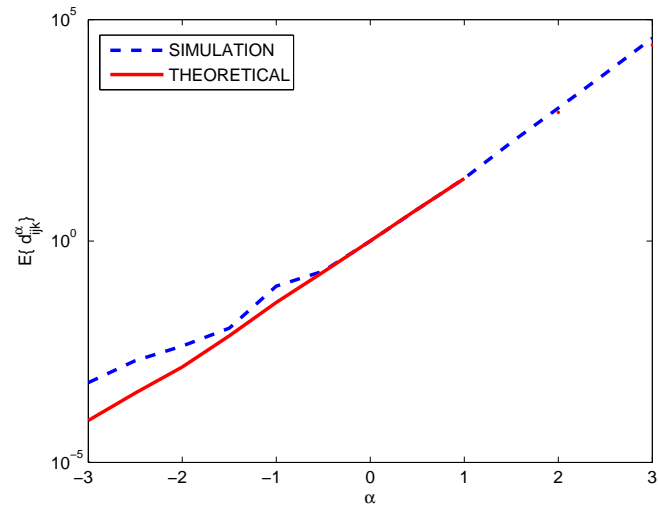


Figure 2.10: Simulation (statistical mean) and analytical result for $E\{d_{ijk}^\alpha\}$ ($i = 10$, $j = 20$ and $k = 5$)

Chapter 3: Interference Modeling in Cognitive Wireless Networks

In cognitive wireless networks, the secondary nodes are required to limit their aggregate interference on the primary nodes. Interference, in general, has a stochastic nature, not only due to randomness in the propagation channel, but also due to the random geographic dispersion of the nodes. In this chapter, we assume primary and secondary nodes in a cognitive radio network form a spatial bivariate Poisson point process. We use the statistical properties of distances in these processes obtained in previous chapter, and seek a statistical representation of interference, in which power levels of the secondary nodes influence the parameters of the model.

3.1 System Model

We consider the deployment of wireless nodes of two qualitatively distinguishable types. The nodes of each type is marginally distributed according to a specific spatial Poisson point process. We distinguish between these nodes as type-P, for primary, and type-S, for secondary (We use the letters P and S, instead of A and B used in Chapter 2).

A general model in which the number of primary and secondary nodes in an area are assumed to be correlated is considered. This assumption is generally valid if the same mechanism that leads to topology formation of the primary network is also involved in the secondary network. This leads to the conclusion that primary and secondary nodes, each having marginal Poisson distribution, are distributed jointly as a bivariate spatial Poisson process.

We consider a single primary node located at the origin. The secondary nodes are then distributed according to a homogeneous Poisson process with conditional intensity of λ_c/π

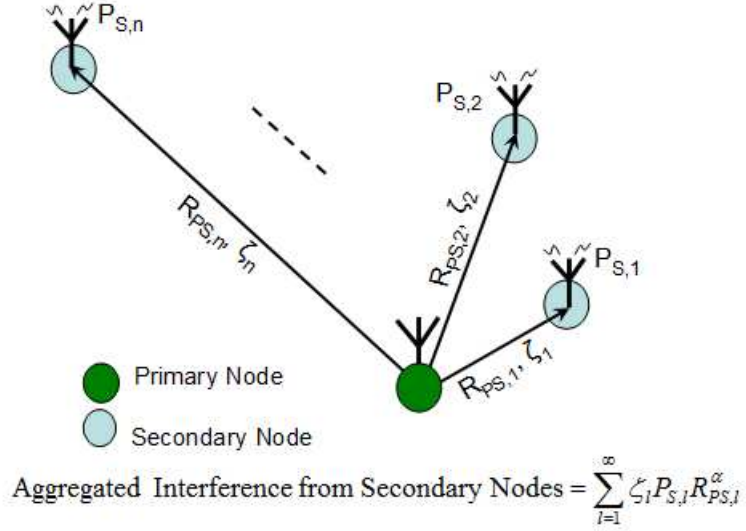


Figure 3.1: Aggregated interference from secondary network to a primary node.

(see the discussion following Lemma 2 in Chapter 2).

3.2 Interference Characterization

Consider a single primary node receiving data on an arbitrary channel. We introduce the following notations:

$R_{PS,l}$: The distance of l th nearest secondary node to the primary node.

$P_{S,l}$: The transmitted power of l th nearest secondary node on the channel.

I_P : The interference due to the nodes of the primary network only.

ξ_l : A σ_s dB log-normal shadow fading component between l th nearest secondary node and the primary node. The first and second moments of ξ are found as

$$E\{\xi\} = e^{\sigma_s^2/2},$$

$$E\{\xi^2\} = e^{2\sigma_s^2},$$

where, $\sigma_s = \sigma_s \frac{\ln 10}{10}$ [38] and $\{\xi_l\}$ are assumed to be i.i.d. random variables.

We consider the following average path loss model:

$$\overline{P_R} = P_T r^\alpha, \quad (3.1)$$

where $\overline{P_R}$ is the average received power, P_T is the transmitted power, r is the distance between transmitter and receiver, and α is a negative real number which represents exponential decaying of power. $-\alpha$ is usually called *path loss exponent*. This model can be further extended to account for a fading component. In this chapter, we consider Log-normal shadow fading. So we have,

$$P_R = \xi P_T r^\alpha. \quad (3.2)$$

Using the above model, $\xi_l P_{S,l} R_{P,S,l}^\alpha$ is the received interference from the l -th nearest secondary transmitter. Defining

$$I \triangleq \sum_{l=1}^{\infty} \xi_l P_{S,l} R_{P,S,l}^\alpha, \quad (3.3)$$

(see Figure 3.1) the total interference at the primary node can be written as

$$I_{tot} = I_P + I. \quad (3.4)$$

The aggregate interference is obviously a random variable. The interference constraint at the primary node can be written as:

$$Pr\{I_{tot} > I_{P,max}\} \leq \epsilon \quad (3.5)$$

where $(I_{P,max}, \epsilon)$ are system-defined values.

(3.5) can be rewritten as

$$P_{exc} \triangleq Pr\{I > \eta\} \leq \epsilon \quad (3.6)$$

where P_{exc} is defined as the probability of excess interference at the primary node. η is the maximum aggregated interference that secondary network can inflict on a primary node ($\eta = I_{P,max} - I_P$).

Note that I , defined in (3.3), is an infinite random series. One may wonder: what conditions should hold in order the summation for I to converge¹ and also the interference constraint be satisfied? In following sections, we seek to model/approximate I as a random variable. In order to satisfy the interference constraint in (3.6), we also need to obtain closed form solution/bounds for its Complementary Cumulative Distribution Function (CCDF) of I .

3.3 Approximation as a Normal Random Variable

We assume that ξ_l is independent from ξ_k (for $l \neq k$) and also from $R_{PS,k}$. Considering the aggregation process in (3.3), the first easy and fast solution for modeling I , seems to be using the central limit theorem and modeling I as a Normal random variable.

If we assume that the Normal assumption for I is correct, then it can be completely characterized by its mean and variance. The mean and variance of I are readily found as

$$\begin{aligned} E\{I\} &= E\{\xi\} \sum_{l=1}^{\infty} P_{S,l} E\{R_{PS,l}^{\alpha}\}, \\ \text{var}\{I\} &= \sum_{l=1}^{\infty} \sum_{k=1}^{\infty} P_{S,l} P_{S,k} \text{cov}\{\xi_l R_{PS,l}^{\alpha}, \xi_k R_{PS,k}^{\alpha}\}. \end{aligned} \quad (3.7)$$

¹Note that, by convergence, we mean the convergence of a random variable.

With I , having a Normal distribution, we have

$$P_{exc} = \frac{1}{2} \operatorname{erfc} \left(\frac{\eta - E\{I\}}{\sqrt{2\operatorname{Var}\{I\}}} \right). \quad (3.8)$$

While $E\{I\}$ can be derived using the $E\{R_{PS,l}^\alpha\}$ found in Chapter 2, for $\operatorname{var}\{I\}$, the covariance can not be found in closed form as we need to have the joint statistics of $R_{PS,l}$ and $R_{PS,k}$. So, we need to resort to the bounds.

Lemma 7. : For $E\{I\}$ upper bounded by E and $\operatorname{var}\{I\}$, upper bounded by V , we have $P_{exc} \leq \epsilon$ if $E + h\sqrt{2V} \leq \eta$, where $\operatorname{erfc}(h) = 2\epsilon$.

Proof. For $P_{exc} \leq \epsilon$ to hold, using (3.8), we need to have $\frac{\eta - E\{I\}}{\sqrt{2\operatorname{var}\{I\}}} \geq \operatorname{erfc}^{-1}(2\epsilon)$. If $E\{I\} < E$ and $\operatorname{var}\{I\} \leq V$, it is sufficient that $E + h\sqrt{2V} \leq \eta$ ($\operatorname{erfc}(h) = 2\epsilon$) in order to have $P_{exc} \leq \epsilon$. \square

3.3.1 Upper bound for $\operatorname{var}\{I\}$

Using the Cauchy-Schwartz inequality,

$$\operatorname{Cov}\{A, B\} \leq \sqrt{\operatorname{Var}\{A\}\operatorname{Var}\{B\}}, \quad (3.9)$$

we can upper-bound the $\operatorname{var}\{I\}$ in (3.7) as

$$\operatorname{var}\{I\} \leq \left[\sum_{l=1}^{\infty} P_{S,l} \sqrt{\operatorname{var}\{\xi_l R_{PS,l}^\alpha\}} \right]^2. \quad (3.10)$$

We also have,

$$\operatorname{var}\{\xi_l R_{PS,l}^\alpha\} = E\{\xi^2\}E\{R_{PS,l}^{2\alpha}\} - E^2\{\xi\}E^2\{R_{PS,l}^\alpha\}. \quad (3.11)$$

For practical values for the parameter, second term above is much smaller than the first term. So,

$$\text{var}\{\xi_l R_{PS,l}^\alpha\} \leq E\{\xi^2\}E\{R_{PS,l}^{2\alpha}\}, \quad (3.12)$$

is a tight bound. Using (3.12) in (3.10), we have

$$\text{var}\{I\} \leq E\{\xi^2\} \left[\sum_{l=1}^{\infty} P_{S,l} \sqrt{E\{R_{PS,l}^{2\alpha}\}} \right]^2. \quad (3.13)$$

Using the results for $E\{R_{PS,l}^\alpha\}$ obtained in Chapter 2, we can find the upper bound of $\text{var}\{I\}$ (i.e., V).

3.4 Approximation as the Sum of a Normal and Log-normal Random Variables

The Gaussian assumption for I , makes it easy to characterize the interference, as it suffices to find the first and second moments only. Although, the use of central limit theorem for the sum of an infinite number of random variables is quite common, nevertheless, to be mathematically precise, the application of CLT is not completely justifiable in this particular problem. The reason is that the variables $R_{PS,n}$ are not independent (i.e., the condition $R_{PS,i} \perp R_{PS,j}$, $i \neq j$ do not hold).

We rewrite I as

$$I = \sum_{i=1}^{\infty} \xi_i P_{S,i} y_i^{\alpha/2}, \quad (3.14)$$

where $y_i = R_{PS,i}^2$. From Lemma 3 in Chapter 2, we have, y_1 and $y_i - y_{i-1}$, $i > 1$ are i.i.d.

exponential random variables with parameter λ_c , and, therefore

$$y_i = y_1 + y_2 - y_1 + \cdots y_i - y_{i-1},$$

is sum of i i.i.d. exponential random variables. Therefore, it has an Erlang distribution with mean $\frac{i}{\lambda_c}$. Since y_i is sum of i i.i.d. exponential random variables we can use the law of large numbers (LLN). Using LLN, we have, for large i , $y_i \rightarrow \frac{i}{\lambda_c}$ almost surely. This can also be seen from

$$\begin{aligned} \frac{\sqrt{\text{Var}\{y_i\}}}{E\{y_i\}} &= \frac{\sqrt{i/\lambda_c^2}}{i/\lambda_c} \\ &= \frac{1}{\sqrt{i}} \rightarrow 0 \quad \text{for large } i \end{aligned} \quad (3.15)$$

Note that mean and variance of y_i are i/λ_c and i/λ_c^2 respectively. For large i , y_i acts like a constant and can be replaced by its mean. So, for N large enough, we can write

$$I \rightarrow \sum_{i=1}^N \xi_i P_{S,i} R_{P_{S,i}}^\alpha + \sum_{i=N+1}^{\infty} \xi_i P_{S,i} \left(\frac{i}{\lambda_c}\right)^{\alpha/2}. \quad (3.16)$$

By defining $I_1 = \sum_{i=1}^N \xi_i P_{S,i} R_{P_{S,i}}^\alpha$ and $I_2 = \sum_{i=N+1}^{\infty} \xi_i P_{S,i} \left(\frac{i}{\lambda_c}\right)^{\alpha/2}$, we can invoke central limit theorem to approximate I_2 as a Normal random variable as it is sum of infinite independent log-normal random variables (i.e., $I_2 \rightarrow \tilde{I}_2 \sim \mathcal{N}(\mu_2, \sigma_2)$). The mean and variance of \tilde{I}_2 can be readily found as

$$\mu_2 = E\{\tilde{I}_2\} = \frac{E\{\xi\}}{\lambda_c^{\alpha/2}} \sum_{i=N+1}^{\infty} P_{S,i} i^{\alpha/2}, \quad (3.17)$$

$$\sigma_2^2 = \text{var}\{\tilde{I}_2\} = \frac{\text{var}\{\xi\}}{\lambda_c^\alpha} \sum_{i=N+1}^{\infty} P_{S,i}^2 i^\alpha. \quad (3.18)$$

It is shown in [39] that linear combination of log-normal random variables of the form $\sum_{i=1}^N A_i \xi_i$, where A_i 's are positive and independent random variables can be approximated by another log-normal random variable. In the summation for I_1 , $\{R_{PS,i}\}$ are not independent. Nevertheless, our simulation results show that log-normal is still a good approximation (see Figure 3.4). So, we can write $I_1 \sim \mathcal{LN}(\mu_1, \sigma_1)$. μ_1 and σ_1^2 are related to $m_1 = E\{I_1\}$ and $s_1^2 = \text{var}\{I_1\}$ [38] as

$$\mu_1 = \ln \left(\frac{m_1^2}{\sqrt{m_1^2 + s_1^2}} \right), \quad (3.19)$$

$$\sigma_1^2 = \ln \left(\left(\frac{s_1}{m_1} \right)^2 + 1 \right). \quad (3.20)$$

m_1 and s_1^2 can be readily found as

$$m_1 = E\{\xi\} \sum_{i=1}^N P_{S,i} E\{R_{PS,i}^\alpha\}, \quad (3.21)$$

$$s_1^2 = \sum_{i=1}^N \sum_{j=1}^N P_{S,i} P_{S,j} \text{cov}\{\xi_i R_{PS,i}^\alpha, \xi_j R_{PS,j}^\alpha\}. \quad (3.22)$$

We assume that $P_{S,i} = p_1$, $1 \leq i \leq N$. In other words, the first N secondary nodes send a fixed power level (i.e., p_1). This will simplify the derivations. Then we have,

$$m_1 = p_1 E\{\xi\} \sum_{i=1}^N E\{R_{PS,i}^\alpha\}. \quad (3.23)$$

To find s_1^2 , we need the joint pdf of $R_{PS,i}$ and $R_{PS,j}$ which is hard to find, so we resort to finding the bounds.

3.4.1 The bounds for s_1^2

Here, we obtain the bounds for s_1^2 as $s_{1,l}^2 \leq s_1^2 \leq s_{1,u}^2$.

$$\begin{aligned} s_1^2 &= \sum_{i=1}^N \sum_{j=1}^N P_{S,i} P_{S,j} \text{cov}\{\xi_i R_{PS,i}^\alpha, \xi_j R_{PS,j}^\alpha\} \\ &= p_1^2 \left\{ \sum_{i=1}^N \text{var}\{\xi_i R_{PS,i}^\alpha\} + \sum_{i=1}^N \sum_{j=1, j \neq i}^N \text{cov}\{\xi_i R_{PS,i}^\alpha, \xi_j R_{PS,j}^\alpha\} \right\} \end{aligned} \quad (3.24)$$

After simplification, we will have

$$s_1^2 = p_1^2 C + p_1^2 E^2\{\xi\} \sum_{i=1}^N \sum_{j=1, j \neq i}^N E\{R_{PS,i}^\alpha R_{PS,j}^\alpha\}, \quad (3.25)$$

where

$$C = E\{\xi^2\} \sum_{i=1}^N E\{R_{PS,i}^{2\alpha}\} - E^2\{\xi\} \left\{ \sum_{i=1}^N E\{R_{PS,i}^\alpha\} \right\}^2. \quad (3.26)$$

So, to find the bounds for s_1^2 , it suffices to find the bounds for $E\{R_{PS,i}^\alpha R_{PS,j}^\alpha\}$. We can use Cauchy-Schwartz inequality to find an upper bound as

$$E\{R_{PS,i}^\alpha R_{PS,j}^\alpha\} \leq \sqrt{E\{R_{PS,i}^{2\alpha}\} E\{R_{PS,j}^{2\alpha}\}}. \quad (3.27)$$

The lower bound can also be found using the Jensen's inequality (note that $f(X) = X^\alpha$ is a convex function for $\alpha < 0$) as

$$E\{R_{PS,i}^\alpha R_{PS,j}^\alpha\} = E\{y_i^{\alpha/2} y_j^{\alpha/2}\} > [E\{y_i y_j\}]^{\alpha/2} \quad (3.28)$$

For $j > i$, we have

$$\begin{aligned}
E\{y_i y_j\} &= E\{y_i(y_i + y_{i+1} - y_i + y_{i+2} - y_{i+1} + \cdots + y_j - y_{j-1})\} \\
&= E\{y_i^2\} + E\{y_i(y_{i+1} - y_i)\} + \cdots + E\{y_i(y_j - y_{j-1})\} \\
&= E\{R_{PS,i}^4\} + (j - i)E\{y_i\}E\{y_{i+1} - y_i\} \\
&= \frac{i(i+1)}{\lambda_c^2} + \frac{(j-i)i}{\lambda_c^2} \\
&= \frac{i(j+1)}{\lambda_c^2}, \tag{3.29}
\end{aligned}$$

which is found using the fact that y_i is Erlang distributed with mean i/λ_c and $y_i \perp (y_k - y_{k-1})$, $k > i$ (See the discussion after Lemma 3 in Chapter 2). For $j < i$, using symmetry, we will have

$$E\{y_i y_j\} = \frac{j(i+1)}{\lambda_c^2}. \tag{3.30}$$

Using the above results in (3.25), we find

$$s_{1,l}^2 = p_1^2 C + p_1^2 E^2\{\xi\} \sum_{i=1}^N \left\{ \sum_{j=1}^{i-1} \frac{[i(j+1)]^{\alpha/2}}{\lambda_c^\alpha} + \sum_{j=i+1}^N \frac{[j(i+1)]^{\alpha/2}}{\lambda_c^\alpha} \right\}, \tag{3.31}$$

$$s_{1,u}^2 = p_1^2 C + p_1^2 E^2\{\xi\} \sum_{i=1}^N \sum_{j=1, j \neq i}^N \sqrt{E\{R_{PS,i}^{2\alpha}\} E\{R_{PS,j}^{2\alpha}\}} \tag{3.32}$$

3.4.2 The CCDF of I

Using these bounds, and replacing $s_{1,l}^2$ in (3.19) and (3.20), we can find $(\mu_{1,u}, \sigma_{1,u}^2)$, upper bounds for μ_1 and σ_1^2 . The lower bounds $(\mu_{1,l}, \sigma_{1,l}^2)$ can also be found by replacing $s_{1,u}^2$ in (3.19) and (3.20).

We have found $I \rightarrow I_1 + \tilde{I}_2$, with $I_1 \sim \mathcal{LN}(\mu_1, \sigma_1)$, and $\tilde{I}_2 \sim \mathcal{N}(\mu_2, \sigma_2)$ and $I_1 \perp \tilde{I}_2$. Using these distributions, we have ²

$$\begin{aligned}
Pr\{I > \eta\} &= \int_0^\infty Pr\{I_1 + \tilde{I}_2 > \eta | I_1 = x\} f_{I_1}(x) dx \\
&= \int_0^\infty Pr\{\tilde{I}_2 > \eta - x\} f_{I_1}(x) dx \\
&= \int_0^\infty Q\left(\frac{\eta - x - \mu_2}{\sigma_2}\right) f_{I_1}(x) dx \\
&= E\left\{Q\left(\frac{\eta - I_1 - \mu_2}{\sigma_2}\right)\right\}. \tag{3.33}
\end{aligned}$$

The expectation of the above Q function dose not have a closed form solution and we need to use numerical integration or resort to bounds and satisfy the interference constraint (see equation (3.6)), by keeping the upper bound less than the threshold (i.e., ϵ).

3.4.3 Approach one

Using integration by substitution in (3.33) with $u = \frac{\ln x - \mu_1}{\sqrt{2}\sigma_1}$, after simplification, we will have

$$\begin{aligned}
Pr\{I > \eta\} &= \int_{-\infty}^\infty \frac{1}{\sqrt{\pi}} Q\left(\frac{\eta - \mu_2 - e^{\mu_1 + \sqrt{2}\sigma_1 u}}{\sigma_2}\right) e^{-u^2} du \\
&\approx \sum_{i=1}^M w_i f^*(u_i) \tag{3.34}
\end{aligned}$$

²Note that, here, we use an extended version of Q function, the range of which also includes negative values. For $x > 0$, $Q(x)$ is the tail probability of $\mathcal{N}(0, 1)$ and for $x < 0$, $Q(x) = 1 - Q(-x)$. We use this extended version because for $x > \eta - \mu_2$, the argument of $Q\left(\frac{\eta - x - \mu_2}{\sigma_2}\right)$ is negative.

where,

$$f^*(u) \triangleq \frac{1}{\sqrt{\pi}} Q \left(\frac{\eta - \mu_2 - e^{\mu_1 + \sqrt{2}\sigma_1 u}}{\sigma_2} \right) \quad (3.35)$$

and we have used the Gauss-Hermite quadrature method. In numerical analysis, we have

$$\int_{-\infty}^{\infty} e^{-x^2} f(x) dx = \sum_{i=1}^M w_i f(x_i) + R_M, \quad (3.36)$$

where M is the number of sample points used for integration. The larger the value of M , the closer will be the approximation. The abscissa (x_i) is the i th zero of the Hermite polynomial $H_M(x)$ ($i = 1, 2, \dots, M$) and the weights (w_i) are given by

$$w_i = \frac{2^{M-1} M! \sqrt{\pi}}{M^2 [H_{M-1}(x_i)]^2}. \quad (3.37)$$

x_i and w_i for different values of M are tabulated in [37].

If we define

$$f_u^*(x) \triangleq \frac{1}{\sqrt{\pi}} Q \left(\frac{\eta - \mu_2 - e^{\mu_{1,u} + \sqrt{2}\sigma_{1,u} x}}{\sigma_2} \right), \quad (3.38)$$

we have $f^*(x) < f_u^*(x)$, for every x . So, we can write

$$Pr\{I > \eta\} < \sum_{i=1}^M w_i f_u^*(x_i). \quad (3.39)$$

3.4.4 Approach two

We have

$$Q\left(\frac{\eta - \mu_2 - x}{\sigma_2}\right) \leq Q\left(\frac{\eta - \mu_2}{\sigma_2}\right) + \frac{0.5 - Q\left(\frac{\eta - \mu_2}{\sigma_2}\right)}{\eta - \mu_2}x, \quad 0 \leq x \leq \eta - \mu_2, \quad (3.40)$$

which is the line connecting the points $(0, Q\left(\frac{\eta - \mu_2}{\sigma_2}\right))$ and $(\eta - \mu_2, 0.5)$ (see Figure 3.2).

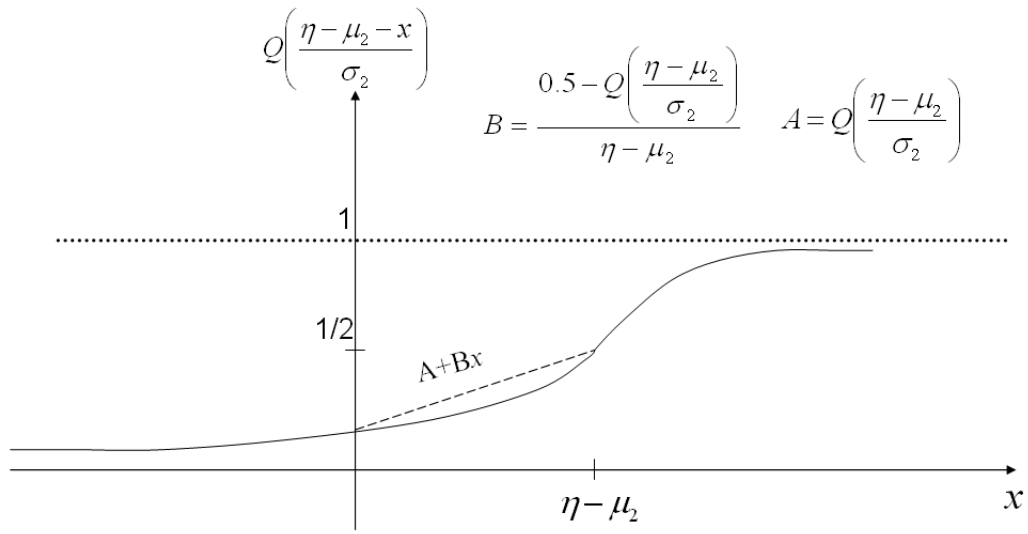


Figure 3.2: Convexity of $Q\left(\frac{\eta - \mu_2 - x}{\sigma_2}\right)$

So we can write

$$Pr\{I > \eta\} < \int_0^{\eta - \mu_2} (A + Bx)f_{I_1}(x) dx + \int_{\eta - \mu_2}^{\infty} Q\left(\frac{\eta - \mu_2 - x}{\sigma_2}\right) f_{I_1}(x) dx \quad (3.41)$$

where $A = Q\left(\frac{\eta - \mu_2}{\sigma_2}\right)$ and $B = \frac{0.5 - Q\left(\frac{\eta - \mu_2}{\sigma_2}\right)}{\eta - \mu_2}$.

Lemma 8. : $Q\left(\frac{\eta - \mu_2 - x}{\sigma_2}\right)$ is concave for $x \geq \eta - \mu_2$ and convex for $x < \eta - \mu_2$.

Proof. Defining

$$G(x) = Q\left(\frac{\eta - \mu_2 - x}{\sigma_2}\right) = \int_{\frac{\eta - \mu_2 - x}{\sigma_2}}^{\infty} \frac{1}{\sqrt{2\pi}} e^{-y^2/2} dy, \quad (3.42)$$

the first and second derivative will be

$$\begin{aligned} G'(x) &= \frac{1}{\sqrt{2\pi}\sigma_2} e^{-\frac{(\eta - \mu_2 - x)^2}{2\sigma_2^2}}, \\ G''(x) &= \frac{1}{\sqrt{2\pi}} \frac{\eta - \mu_2 - x}{\sigma_2^2} e^{-\frac{(\eta - \mu_2 - x)^2}{2\sigma_2^2}}. \end{aligned} \quad (3.43)$$

So, we have $G''(x) > 0$ for $x < \eta - \mu_2$ and $G''(x) < 0$ for $x > \eta - \mu_2$. \square

If we define the random variable \check{I}_1 such that

$$f_{\check{I}_1}(x) \triangleq \begin{cases} \frac{f_{I_1}(x)}{F_{c,I_1}(\eta - \mu_2)}, & x > \eta - \mu_2 \\ 0, & \text{o.w.} \end{cases}$$

then we have,

$$\begin{aligned} \int_{\eta - \mu_2}^{\infty} Q\left(\frac{\eta - \mu_2 - x}{\sigma_2}\right) f_{I_1}(x) dx &= F_{c,I_1}(\eta - \mu_2) \int_{\eta - \mu_2}^{\infty} Q\left(\frac{\eta - \mu_2 - x}{\sigma_2}\right) f_{\check{I}_1}(x) dx \\ &= Q\left(\frac{\ln(\eta - \mu) - \mu_1}{\sigma_2}\right) E\left\{Q\left(\frac{\eta - \mu_2 - \check{I}_1}{\sigma_2}\right)\right\} \\ &\leq Q\left(\frac{\ln(\eta - \mu) - \mu_1}{\sigma_2}\right) Q\left(\frac{\eta - \mu_2 - E\{\check{I}_1\}}{\sigma_2}\right) \end{aligned} \quad (3.44)$$

The inequality above is found from Jensen's inequality, using the fact that $Q\left(\frac{\eta - \mu_2 - x}{\sigma_2}\right)$ is

concave for $x \geq \eta - \mu_2$. $E\{\check{I}_1\}$ can be readily found as

$$E\{\check{I}_1\} = e^{\mu_1 + \frac{\sigma_1^2}{2}} \cdot \frac{Q\left(\frac{\ln(\eta - \mu_2) - (\mu_1 + \sigma_1^2)}{\sigma_1}\right)}{Q\left(\frac{\ln(\eta - \mu_2) - \mu_1}{\sigma_1}\right)}. \quad (3.45)$$

The first integral can also be found as

$$\begin{aligned} \int_0^{\eta - \mu_2} (A + Bx)f_{I_1}(x) dx = & A \left(1 - Q\left(\frac{\ln(\eta - \mu_2) - \mu_1}{\sigma_1}\right)\right) \\ & + B e^{\mu_1 + \sigma_1^2/2} \left(1 - Q\left(\frac{\ln(\eta - \mu_2) - (\mu_1 + \sigma_1^2)}{\sigma_1}\right)\right) \end{aligned} \quad (3.46)$$

Putting together equations (38)-(41) and using appropriate bounds for μ_1 and σ_1 , we find following upper bound for $Pr\{I > \eta\}$

$$\begin{aligned} Pr\{I > \eta\} < & Q\left(\frac{\eta - \mu_2}{\sigma_2}\right) \left(1 - Q\left(\frac{\ln(\eta - \mu_2) - \mu_{1,l}}{\sigma_{1,l}}\right)\right) \\ & + \frac{0.5 - Q\left(\frac{\eta - \mu_2}{\sigma_2}\right)}{\eta - \mu_2} \cdot e^{\mu_{1,u} + \frac{\sigma_{1,u}^2}{2}} \left(1 - Q\left(\frac{\ln(\eta - \mu_2) - (\mu_{1,l} + \sigma_{1,l}^2)}{\sigma_{1,l}}\right)\right) \\ & + Q\left(\frac{\ln(\eta - \mu_2) - \mu_{1,u}}{\sigma_{1,u}}\right) \cdot Q\left(\frac{\eta - \mu_2 - E_u\{\check{I}_1\}}{\sigma_2}\right). \end{aligned} \quad (3.47)$$

Here, $E_u\{\check{I}_1\}$ is an upper bound for $E\{\check{I}_1\}$ (to maximize the Q function) and is found from (3.45) as

$$E_u\{\check{I}_1\} = e^{\mu_{1,u} + \frac{\sigma_{1,u}^2}{2}} \cdot \frac{Q\left(\frac{\ln(\eta - \mu_2) - (\mu_{1,u} + \sigma_{1,u}^2)}{\sigma_{1,u}}\right)}{Q\left(\frac{\ln(\eta - \mu_2) - \mu_{1,l}}{\sigma_{1,l}}\right)}. \quad (3.48)$$

3.5 Interference Modeling with Traffic Considerations

In previous sections, we have implicitly assumed that the secondary nodes always have some data to transmit and the primary node is always in the receiving mode. In practice, however, the statistical properties of interference are influenced by the traffic statistics.

In this section, we consider a simple traffic model based on the M/M/1/1 queueing model. We define the random processes

$$\phi_l(t) \triangleq \begin{cases} 1, & \text{if } l\text{th nearest secondary node is busy at time } t \\ 0, & \text{if } l\text{th nearest secondary node is idle at time } t \end{cases} \quad (3.49)$$

We assume that the probabilities of a node being busy and idle are Δ and $1 - \Delta$ respectively. Assuming that nodes operate as M/M/1/1 queues, $\phi_l(t)$ is a stationary ergodic continuous-time Markov process and in the steady state, $\Delta = \frac{\rho}{1+\rho}$, where ρ is the traffic intensity (i.e., the ratio of arrival rate to service rate). The aggregated interference in (3.3), will then be time-dependent (i.e., a random process) and is written as,

$$I(t) = \sum_{l=1}^{\infty} \phi_l(t) P_{S,l} \xi_l R_{PS,l}^{\alpha}. \quad (3.50)$$

Note that the effective transmitted power by l th nearest secondary node is $\phi_l(t) P_{S,l}$. $\phi_l(t)$ is assumed to be independent from ξ_k and $R_{PS,n}$.

Similar to $\phi_l(t)$, we can define

$$\varphi(t) \triangleq \begin{cases} 1, & \text{if the primary node is receiving data at time } t \\ 0, & \text{if the primary node is not receiving data at time } t \end{cases} \quad (3.51)$$

and assume that the probability of the primary node being in the receiving mode is Π . Π is dependent on the topology, routing method and traffic statistics in the primary network,

among other factors. We also assume that $\varphi(t)$ is a stationary process.

The interference constraint defined in (3.6) can be modified to account for the traffic statistics. We define the probability of collision, $P_c(t)$, as the probability of aggregated interference from secondary network being larger than η while the primary node being in the receiving mode. The interference constraint can then be written as,

$$P_c(t) \leq \epsilon. \quad (3.52)$$

$P_c(t)$ can be found as

$$\begin{aligned} P_c(t) &= \Pr\{\text{collision}|\varphi(t) = 0\}\Pr\{\varphi(t) = 0\} + \Pr\{\text{collision}|\varphi(t) = 1\}\Pr\{\varphi(t) = 1\} \\ &= \Pr\{I(t) \geq \eta\} \end{aligned} \quad (3.53)$$

Similar to the previous sections, we consider two different models for interference.

3.5.1 Interference as a Normal Random Process

Again, we first assume that central limit theorem can be applied and $I(t)$ can be approximated as a Gaussian random process. It is easy to see that

$$E\{I(t)\} = \Delta E\{I\} \quad (3.54)$$

$$\text{var}\{I(t)\} = \sum_{i=1}^{\infty} \sum_{j=1}^{\infty} P_{S,i} P_{S,j} \text{cov}\{\phi_i(t)\xi_i R_{PS,i}^{\alpha}, \phi_j(t)\xi_j R_{PS,j}^{\alpha}\} \quad (3.55)$$

Following the same approach in Subsection 3.3.1, we have

$$\begin{aligned} \text{var}\{I(t)\} &\leq \left[\sum_{l=1}^{\infty} P_{S,l} \sqrt{E\{\phi^2(t)\} E\{\xi^2\} E\{R_{PS,l}^{2\alpha}\}} \right]^2 \\ &= \Delta E\{\xi^2\} \left[\sum_{l=1}^{\infty} P_{S,l} \sqrt{E\{R_{PS,l}^{2\alpha}\}} \right]^2 \end{aligned} \quad (3.56)$$

Lemma 9. : For $E\{I(t)\}$ and $\text{var}\{I(t)\}$ upper-bounded by E' and V' respectively, we have $P_c(t) \leq \epsilon$ if $E' + h'\sqrt{2V'} \leq \eta$ where $\text{erfc}(h') = 2\frac{\epsilon}{\Pi}$.

Proof. From (3.53), we need to have $\Pr\{I(t) \geq \eta\} \leq \frac{\epsilon}{\Pi}$ or $\frac{\eta - E\{I(t)\}}{\sqrt{2\text{var}\{I(t)\}}} \geq \text{erfc}^{-1}(2\frac{\epsilon}{\Pi})$. If $E\{I(t)\} \leq E'$ and $\text{var}\{I(t)\} \leq V'$, it is sufficient that $E' + h'\sqrt{2V'} \leq \eta$ ($\text{erfc}(h') = 2\frac{\epsilon}{\Pi}$) in order to have $P_{exc} \leq \epsilon$. \square

3.5.2 Sum of Normal and Log-normal Assumption

Using the same approach as in Section 3.4, we can split the aggregate interference and use the law of large numbers to write

$$I(t) \rightarrow \sum_{i=1}^N \phi_i(t) \xi_i P_{S,i} R_{P_{S,i}}^\alpha + \sum_{i=N+1}^{\infty} \phi_i(t) \xi_i P_{S,i} \left(\frac{i}{\lambda_c}\right)^{\alpha/2}. \quad (3.57)$$

We can again approximate the first summation as a Log-normal and the second one as a Normal random variable. Denoting the mean and variance of the Normal random variable as $\dot{\mu}_2$ and $\dot{\sigma}_2^2$, we have

$$\begin{aligned} \dot{\mu}_2 &= \frac{E\{\phi(t)\xi\}}{\lambda_c^{\alpha/2}} \sum_{i=N+1}^{\infty} P_{S,i} \cdot i^{\alpha/2} \\ &= \frac{\Delta E\{\xi\}}{\lambda_c^{\alpha/2}} \sum_{i=N+1}^{\infty} P_{S,i} \cdot i^{\alpha/2}, \end{aligned} \quad (3.58)$$

and,

$$\begin{aligned} \dot{\sigma}_2^2 &= \frac{\text{var}\{\phi(t)\xi\}}{\lambda_c^\alpha} \sum_{i=N+1}^{\infty} P_{S,i}^2 \cdot i^\alpha \\ &= \frac{E\{\xi^2\}\Delta - E^2\{\xi\}\Delta^2}{\lambda_c^\alpha} \sum_{i=N+1}^{\infty} P_{S,i}^2 \cdot i^\alpha. \end{aligned} \quad (3.59)$$

Denoting the mean and variance of the Log-normal random variable as \hat{m}_1 and \hat{s}_1^2 respectively, and with $P_{S,i} = p_1$, $1 \leq i \leq N$, we have

$$\begin{aligned}\hat{m}_1 &= p_1 E\{\xi\} E\{\phi(t)\} \sum_{i=1}^N E\{R_{P_{S,i}}^\alpha\} \\ &= p_1 \Delta E\{\xi\} \sum_{i=1}^N E\{R_{P_{S,i}}^\alpha\}\end{aligned}\quad (3.60)$$

and,

$$\hat{s}_1^2 = p_1^2 \sum_{i=1}^N \sum_{j=1}^N \text{cov}\{\xi_i \phi_i(t) R_{P_{S,i}}^\alpha, \xi_j \phi_j(t) R_{P_{S,j}}^\alpha\}.\quad (3.61)$$

Using the same approach as in Section 3.4.1, we can find bounds for \hat{s}_1^2 as $\hat{s}_{1,l}^2 < \hat{s}_1^2 < \hat{s}_{1,u}^2$, where

$$\hat{s}_{1,l}^2 = p_1^2 \dot{C} + p_1^2 E^2\{\xi\} \Delta^2 \sum_{i=1}^N \left\{ \sum_{j=1}^{i-1} \frac{[i(j+1)]^{\alpha/2}}{\lambda_c^\alpha} + \sum_{j=i+1}^N \frac{[j(i+1)]^{\alpha/2}}{\lambda_c^\alpha} \right\},\quad (3.62)$$

$$\hat{s}_{1,u}^2 = p_1^2 \dot{C} + p_1^2 E^2\{\xi\} \sum_{i=1}^N \sum_{j=1, j \neq i}^N \sqrt{E\{R_{P_{S,i}}^{2\alpha}\} E\{R_{P_{S,j}}^{2\alpha}\}},\quad (3.63)$$

$$\dot{C} = \Delta E\{\xi^2\} \sum_{i=1}^N E\{R_{P_{S,i}}^{2\alpha}\} - \Delta^2 E^2\{\xi\} \left\{ \sum_{i=1}^N E\{R_{P_{S,i}}^\alpha\} \right\}^2.\quad (3.64)$$

Using these bounds for \hat{s}_1^2 , lower and upper bounds can be obtained for the parameters of the Log-normal random variable (i.e., $(\hat{\mu}_{1,l}, \hat{\sigma}_{1,l}^2)$ and $(\hat{\mu}_{1,u}, \hat{\sigma}_{1,u}^2)$).

3.6 Simulation Results

We consider a bivariate spatial Poisson process with parameters $\lambda = 0.005$, $\mu = 0.001$, and $\nu = 0.0025$ as we did in Chapter 2. We assume that the secondary nodes have a perfect estimate of these values and thereby λ_c . A disc with radius $R = 1000$ units is considered as the underlying area in which primary and secondary nodes are present. We consider $\sigma^2 = 10$ to satisfy the condition $\sigma^2 \gg 1$. We assume a primary node exists in the origin so that the number of secondary nodes in the area, m , will be a Poisson random variable with mean $\bar{m} = \lambda_c R^2 = (a + bc)R^2 = 25044$.

A $\sigma_s = 6$ dB log-normal shadowing is considered in our simulations, for which we have $\sigma_S \simeq 1.38$.

In Figure 3.3, we examine the accuracy of the Normal assumption in Section 3.3. For simplicity we assume $P_{S,i} = 1$. For $\alpha = -3.2$, we have plotted the normalized histogram and the Normal distribution with mean $E\{I\} = E\{\xi\} \sum_{l=1}^{\infty} E\{R_{P_{S,l}}^{\alpha}\}$ and the upper bound of variance $V = E\{\xi^2\} \left[\sum_{l=1}^{\infty} \sqrt{E\{R_{P_{S,l}}^{2\alpha}\}} \right]^2$ (using (3.13)). It is clear from this figure that the histogram is more right tailed and there is a positive skewness which is not observed in the Normal pdf.

In Figure 3.4, we have plotted the normalized histogram of $I_1 = \sum_{i=1}^N \xi_i P_{S,i} R_{P_{S,i}}^{\alpha}$ for $P_{S,i} = p_1 = 1$, $1 \leq i \leq N$, $N = 1000$ and $\alpha = -3.2$. Alongside, The pdfs of $\mathcal{LN}(\mu_{1,l}, \sigma_{1,l})$ and $\mathcal{LN}(\mu_{1,u}, \sigma_{1,u})$ are plotted. The pdfs are practically the same. This shows that the obtained bounds for s_1^2 (see equations (3.31) and (3.32)) are very close. Also the Log-normal assumption for I_1 is a close approximation.

In Figure 3.5, the normalized histogram of $I_2 = \sum_{i=N+1}^{\infty} \xi_i P_{S,i} R_{P_{S,i}}^{\alpha}$ for $P_{S,i} = 1$, $i > N$, $N = 1000$ and $\alpha = -3.2$ is plotted. This shows that the Normal assumption for I_2 is a close approximation.

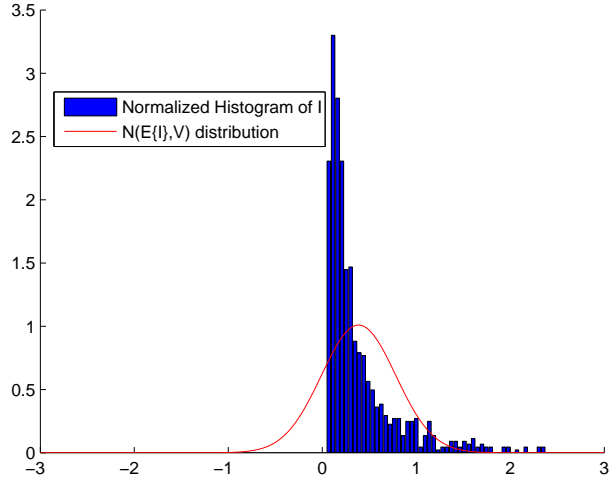


Figure 3.3: Normalized histogram of $I = \sum_{i=1}^{\infty} \xi_i R_{PS,i}^{\alpha}$ and the pdf of the $\mathcal{N}(E\{I\}, V)$.

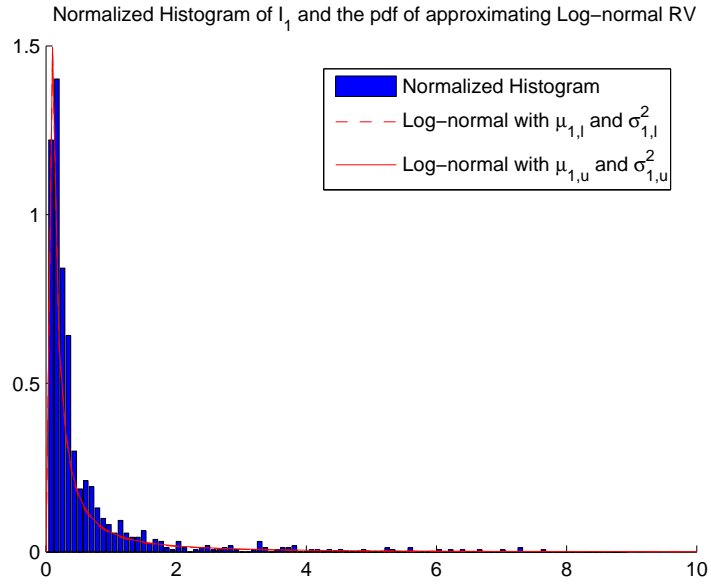


Figure 3.4: The normalized histogram of $I_1 = \sum_{i=1}^N \xi_i P_{S,i} R_{PS,i}^{\alpha}$ for $P_{S,i} = p_1 = 1$, $N = 1000$ and $\alpha = -3.2$ and the pdfs of $\mathcal{LN}(\mu_{1,l}, \sigma_{1,l})$ and $\mathcal{LN}(\mu_{1,u}, \sigma_{1,u})$.

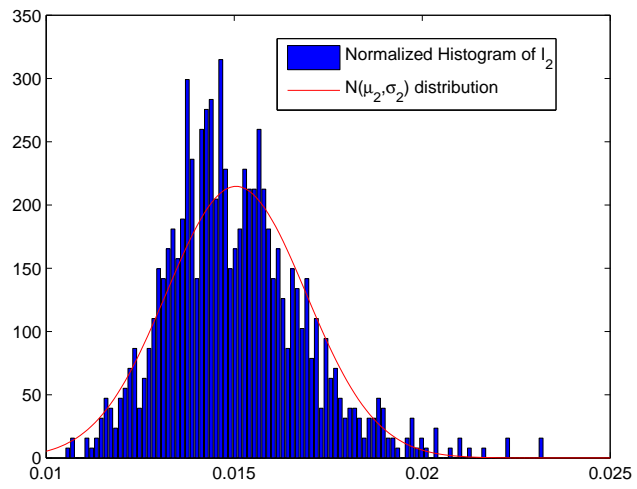


Figure 3.5: Histogram of I_2 and the pdf of $\mathcal{N}(\mu_2, \sigma_2)$

Chapter 4: Power Control for Interference Avoidance in Cognitive Wireless Networks

In Chapter 3, assuming the primary and secondary nodes in a cognitive wireless network form a spatial bivariate Poisson point process, we obtained two different models for characterizing the aggregate interference on a primary node. The first model is based on the Normal assumption of interference assuming that central limit theorem can be applied. The second model is more sophisticated and is based on the sum of a Normal and Log-normal random variables. While the total interference originated from the close neighbors contribute to the Log-normal part, the rest of the nodes are responsible for the Normal random variable. The Log-normal part leads to the distribution of interference being more right-tailed and positively skewed. This observation is also reported in [26] using the cumulants of the aggregate interference.

In both of these models, the parameters depend on the power levels of the secondary neighbors of a primary node. So the power levels of the secondary nodes act as the degrees of freedom, by control of which, the parameters of the models can be adjusted and thereby the interference constraint can be satisfied. In this chapter, we consider each of the developed models separately, and devise power control strategies that ensure interference constraint is satisfied.

4.1 Aggregate interference as a Normal Random Variable

In Section 3.3, Lemma 7, we found that with interference modeled as a Normal random variable, and with the mean and variance of interference upper-bounded by E and V respectively, it is sufficient to have $E + h\sqrt{2V} \leq \eta$ ($\text{erfc}(h) = 2\epsilon$) in order to have $P_{exc} \leq \epsilon$

(i.e., interference constraint satisfied). Furthermore, we found

$$E\{I\} = E\{\xi\} \sum_{l=1}^{\infty} P_{S,l} E\{R_{PS,l}^{\alpha}\}, \quad (4.1)$$

and an upper-bound for $\text{var}\{I\}$ (i.e., V) as

$$V = E\{\xi^2\} \left[\sum_{l=1}^{\infty} P_{S,l} \sqrt{E\{R_{PS,l}^{2\alpha}\}} \right]^2. \quad (4.2)$$

The following upper bound exist for gamma function from [40]:

$$\Gamma(l + \delta) < (l - 1)! l^{\delta}, \quad 0 < \delta < 1, \quad l = 1, 2, \dots \quad (4.3)$$

Using this bound, we have

$$\Gamma(l + \alpha) = \Gamma(l + \lfloor \alpha \rfloor + \alpha - \lfloor \alpha \rfloor) < (l + \lfloor \alpha \rfloor - 1)! (l + \lfloor \alpha \rfloor)^{\alpha - \lfloor \alpha \rfloor}, \quad l = -\lfloor \alpha \rfloor + 1, \dots$$

and for $\alpha < 0$

$$\frac{\Gamma(l + \alpha)}{(l - 1)!} < \frac{1}{(l + \lfloor \alpha \rfloor) \cdots (l - 1)} (l + \lfloor \alpha \rfloor)^{\alpha - \lfloor \alpha \rfloor} < \frac{(l + \lfloor \alpha \rfloor)^{\alpha - \lfloor \alpha \rfloor}}{(l + \lfloor \alpha \rfloor)^{-\lfloor \alpha \rfloor}} = (l + \lfloor \alpha \rfloor)^{\alpha}, \quad l = -\lfloor \alpha \rfloor + 1, \dots \quad (4.4)$$

Using this, we have

$$E\{R_{PS,n}^{\alpha}\} = \frac{\Gamma(l + \alpha/2)}{(l - 1)! \lambda_c^{\alpha/2}} < \frac{(l + \lfloor \alpha/2 \rfloor)^{\alpha/2}}{\lambda_c^{\alpha/2}}, \quad l = -\lfloor \alpha/2 \rfloor + 1, \dots \quad (4.5)$$

Using the above result in (4.1), we obtain

$$\begin{aligned}
E\{I\} &= E\{\xi\} \left[\sum_{l=1}^{-\lfloor \alpha \rfloor} P_{S,l} E\{R_{PS,l}^\alpha\} + \sum_{l=-\lfloor \alpha \rfloor + 1}^{\infty} P_{S,l} \frac{\Gamma(l + \alpha/2)}{(l-1)! \lambda_c^{\alpha/2}} \right] \\
&< E\{\xi\} \left[\sum_{l=1}^{-\lfloor \alpha \rfloor} P_{S,l} E\{R_{PS,l}^\alpha\} + \sum_{l=-\lfloor \alpha \rfloor + 1}^{\infty} P_{S,l} \frac{(l + \lfloor \alpha/2 \rfloor)^{\alpha/2}}{\lambda_c^{\alpha/2}} \right]. \tag{4.6}
\end{aligned}$$

For $\alpha < 0$, $\lfloor \alpha \rfloor < \lfloor \alpha/2 \rfloor$ and the last summation can be further upper bounded to find

$$E = E\{\xi\} \left[\sum_{l=1}^{-\lfloor \alpha \rfloor} P_{S,l} E\{R_{PS,l}^\alpha\} + \sum_{l=-\lfloor \alpha \rfloor + 1}^{\infty} P_{S,l} \frac{(l + \lfloor \alpha \rfloor)^{\alpha/2}}{\lambda_c^{\alpha/2}} \right]. \tag{4.7}$$

We also find, using (4.5) with α replaced by 2α in (4.2),

$$V = E\{\xi^2\} \left[\sum_{l=1}^{-\lfloor \alpha \rfloor} P_{S,l} \sqrt{E\{R_{PS,l}^{2\alpha}\}} + \sum_{l=-\lfloor \alpha \rfloor + 1}^{\infty} P_{S,l} \frac{(l + \lfloor \alpha \rfloor)^{\alpha/2}}{\lambda_c^{\alpha/2}} \right]^2. \tag{4.8}$$

Power levels chosen by secondary neighboring nodes determine whether the infinite series in (4.7) and (4.8) converge. We introduce two power control strategies which lead to the convergence of these summations and also satisfy the constraint of Lemma 3.

4.1.1 Power Control with Constant Power Levels

For $\alpha < -2$ (i.e., path loss exponent $(-\alpha)$ larger than 2 which is practically the case), the infinite series in (4.7) and (4.8) converge for constant power levels. Assume that

$$P_{S,l} = C_1, \quad l = 1, 2, \dots \tag{4.9}$$

From (4.7) and (4.8), we have $E = K_1 C_1$ and $V = K_2 C_1^2$, where K_1 and K_2 are as

$$\begin{aligned} K_1 &= E\{\xi\} \left[\sum_{l=1}^{-[\alpha]} E\{R_{PS,l}^\alpha\} + \frac{1}{\lambda_c^{\alpha/2}} \sum_{l=1}^{\infty} l^{\alpha/2} \right] \\ &= E\{\xi\} \left[\sum_{l=1}^{-[\alpha]} E\{R_{PS,l}^\alpha\} + \frac{1}{\lambda_c^{\alpha/2}} \zeta(-\alpha/2) \right] \end{aligned} \quad (4.10)$$

and

$$\begin{aligned} K_2 &= E\{\xi^2\} \left[\sum_{l=1}^{-[\alpha]} \sqrt{E\{R_{PS,l}^{2\alpha}\}} + \frac{1}{\lambda_c^{\alpha/2}} \sum_{l=1}^{\infty} l^{\alpha/2} \right]^2 \\ &= E\{\xi^2\} \left[\sum_{l=1}^{-[\alpha]} \sqrt{E\{R_{PS,l}^{2\alpha}\}} + \frac{1}{\lambda_c^{\alpha/2}} \zeta(-\alpha/2) \right]^2 \end{aligned} \quad (4.11)$$

where $\zeta(\cdot)$ is the Riemann-Zeta function which is convergent when its argument is larger than 1 ¹ [41]. From Lemma 7 in Chapter 3, C_1 needs to satisfy the inequality $C_1 < \frac{\eta}{K_1 + h\sqrt{2K_2}}$.

4.1.2 Power Control with Distance-dependent Power Levels

A typical $P_{S,l}$ that assures the convergence of the infinite series in (4.7) and (4.8) is

$$P_{S,l} = \begin{cases} k(l + [\alpha])^\beta, & l = -[\alpha] + 1, \dots \\ C_2, & l = 1, \dots, -[\alpha], \end{cases} \quad (4.12)$$

where k , β and C_2 are constants.

¹When defined in the complex domain, we should have $\Re(s) > 1$ for $\zeta(s)$ to converge to an analytic function.

Using this power control strategy, we will have

$$\begin{aligned}
E &= E\{\xi\} \sum_{l=1}^{-[\alpha]} E\{R_{PS,l}^\alpha\} C_2 + \frac{E\{\xi\} \zeta(-\alpha/2 - \beta)}{\lambda_c^{\alpha/2}} k = K'_1 C_2 + K'_2 k, \\
V &= E\{\xi^2\} \left[\sum_{l=1}^{-[\alpha]} \sqrt{E\{R_{PS,l}^{2\alpha}\}} C_2 + \frac{\zeta(-\alpha/2 - \beta)}{\lambda_c^{\alpha/2}} k \right]^2 = K'_3 C_2^2 + K'_4 k^2 + K'_5 C_2 k. \quad (4.13)
\end{aligned}$$

where,

$$\begin{aligned}
K'_1 &= E\{\xi\} \sum_{l=1}^{-[\alpha]} E\{R_{PS,l}^\alpha\}, \\
K'_2 &= \frac{E\{\xi\} \zeta(-\alpha/2 - \beta)}{\lambda_c^{\alpha/2}}, \\
K'_3 &= E\{\xi^2\} \left[\sum_{l=1}^{-[\alpha]} \sqrt{E\{R_{PS,l}^{2\alpha}\}} \right]^2, \\
K'_4 &= E\{\xi^2\} \frac{\zeta^2(-\alpha/2 - \beta)}{\lambda_c^\alpha}, \\
K'_5 &= \frac{2 \sum_{l=1}^{-[\alpha]} E\{R_{PS,l}^{2\alpha}\} \zeta(-\alpha/2 - \beta)}{\lambda_c^{\alpha/2}}. \quad (4.14)
\end{aligned}$$

For the convergence of Zeta function, we need to have $-\alpha/2 - \beta > 1$. Note that for $\alpha < -2$, $-\alpha/2 - 1 > 0$ and we can choose $\beta = -\alpha/2 - 1 - \epsilon$ and set ϵ small enough to make β positive. This will make the power levels steadily increase for $l \geq -[\alpha] + 1$. On the other hand, we may have $\beta < 0$, in which case, the power levels will steadily decrease for $l \geq -[\alpha] + 1$.

It is clear that there is not a unique (C_2, k) pair that satisfy the constraint in Lemma 7 in Chapter 3. Any (C_2, k) in the dashed area of Figure 4.1 satisfies this constraint.

For $C_2 = 0$, the interference constraint reduces to $k \leq \frac{\eta}{h\sqrt{2K'_4 + K'_2}}$. The constant $k =$

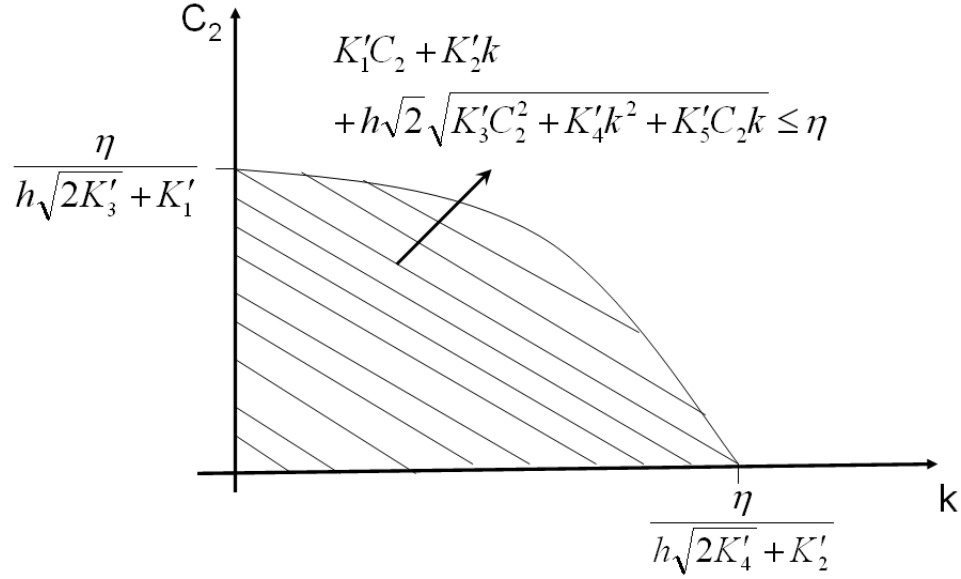


Figure 4.1: The acceptable values for (C_2, k) in (4.12) to satisfy the interference constraint in Lemma 7 in Chapter 3.

$\frac{\eta}{h\sqrt{2K_4'} + K_2'}$ has been plotted for different values of path loss exponent and for the given parameters in Figure 4.2. It can be seen from this figure that, for the given values of parameters, and to reach P_{exc} of around 0.1, the values of k equal to 4×10^{-7} , 1.5×10^{-7} and 0.5×10^{-7} works fine for path loss exponents of 2, 3, and 4, respectively.

Note that all of the above power control strategies work fine to satisfy the interference constraint at the primary receiving node with the given ϵ . The difference between these strategies is that which of the nodes (nodes closer to or further from the primary node or all of them equally) take the responsibility to suppress their power levels more. The second strategy, with power levels increasing with distance, makes more sense, as the further secondary nodes are supposed to be more immune and have more relaxed power constraints.

A secondary node either needs no information of its location with respect to the primary node (the first strategy), or only needs to know where it is located in the sequence of neighboring nodes ordered according to the Euclidean distance to the primary node (second strategy). In other words, it needs to find n if it is the n th nearest neighbor to the primary node. This can be obtained if secondary nodes exchange information on their relative

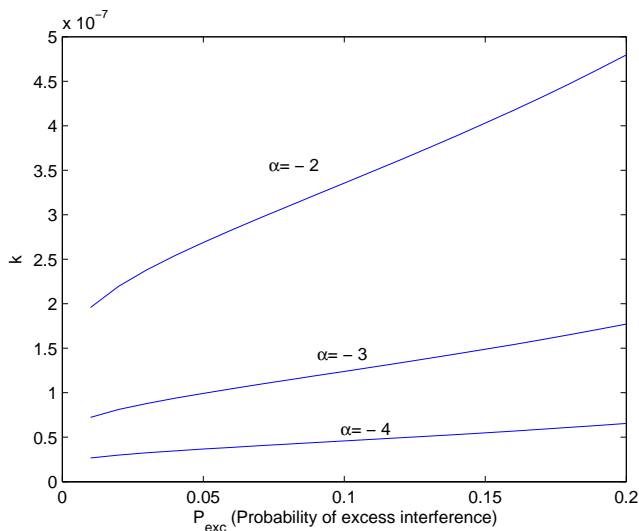


Figure 4.2: Constant k in (4.12), when $C_2 = 0$, $\beta = -\alpha/2 - 1.1$ and for different values of path loss exponent ($\lambda = 1$, $\mu = 2$, $\nu = 0.5$, $\eta = 0$ dBm, and $\sigma^2 \gg 1$).

position to the primary node.

4.2 Aggregate Interference as Sum of a Normal and Log-normal Random Variables

In Section 3.4., we found a more accurate approximation for the aggregate interference to be the sum of a Normal and a Log-normal random variables. With this assumption, we found two upper bounds for the CCDF of this random variable (i.e., probability of excess interference). The expressions are dependent on μ_2 , σ_2 , and upper and lower bounds of μ_1 and σ_1 (i.e., $(\mu_{1,l}, \sigma_{1,l})$ and $(\mu_{1,u}, \sigma_{1,u})$). $(\mu_{1,l}, \sigma_{1,l})$ and $(\mu_{1,u}, \sigma_{1,u})$ are determined by the choice of p_1 , as we assumed $P_{S,i} = p_1$, $1 \geq i \leq N$ (see (3.23), (3.31) and (3.32)). On the other hand μ_2 and σ_2 are infinite summations which depend on the choice of $P_{S,i}$, $i \geq N+1$. In the following Subsections, we consider two different power control strategies which make these summations converge and the interference constraint satisfied.

4.2.1 Fixed Power Levels

For fixed power levels, (i.e., $P_{S,i} = p_2$, $i \geq N + 1$), the equations (3.17) and (3.18) can be written as

$$\begin{aligned}\mu_2 &= \frac{E\{\xi\}p_2}{\lambda_c^{\alpha/2}} \sum_{i=N+1}^{\infty} i^{\alpha/2} \\ &= \frac{E\{\xi\}p_2}{\lambda_c^{\alpha/2}} \left(\zeta(-\alpha/2) - \sum_{i=1}^N i^{\alpha/2} \right),\end{aligned}\quad (4.15)$$

$$\begin{aligned}\sigma_2^2 &= \frac{\text{var}\{\xi\}p_2^2}{\lambda_c^\alpha} \sum_{i=N+1}^{\infty} i^\alpha \\ &= \frac{\text{var}\{\xi\}p_2^2}{\lambda_c^\alpha} \left(\zeta(-\alpha) - \sum_{i=1}^N i^\alpha \right).\end{aligned}\quad (4.16)$$

In a practical path loss models, we always have $\alpha \leq -2$ with equality for the free space model. So, μ_2 and σ_2^2 are convergent even with fixed power levels. In this case, the degrees of freedom are the parameters p_1 and p_2 . Based on which upper bound we use for P_{exc} , (3.39) or (3.47), p_1 and p_2 are determined such that the interference constraint is satisfied.

4.2.2 Distance-dependent Power Levels

A typical $P_{S,i}$, that assures the convergence of the series in (3.17) and (3.18) is

$$P_{S,i} = ki^\beta, \quad i \geq N + 1 \quad (4.17)$$

where k and β are constant and $\beta < -\alpha/2 - 1$. In this case,

$$\begin{aligned}\mu_2 &= \frac{E\{\xi\}k}{\lambda_c^{\alpha/2}} \sum_{i=N+1}^{\infty} i^{\alpha/2+\beta} \\ &= \frac{E\{\xi\}k}{\lambda_c^{\alpha/2}} \left(\zeta(-\alpha/2 - \beta) - \sum_{i=1}^N i^{\alpha/2+\beta} \right),\end{aligned}\tag{4.18}$$

$$\begin{aligned}\sigma_2^2 &= \frac{k^2 \text{var}\{\xi\}}{\lambda_c^\alpha} \sum_{i=N+1}^{\infty} i^{\alpha+2\beta} \\ &= \frac{k^2 \text{var}\{\xi\}}{\lambda_c^\alpha} \left(\zeta(-\alpha/2 - \beta) - \sum_{i=1}^N i^{\alpha+2\beta} \right).\end{aligned}\tag{4.19}$$

Note that for $\alpha < -2$, $-\alpha/2 - 1 > 0$ and β can be chosen either positive or negative, which correspond to power levels steadily increasing or decreasing for $i \geq N + 1$. In this case, the degrees of freedom are p_1 , k and β , which should be adjusted such that the interference constraint is satisfied using the upper bound (3.39) or (3.47).

4.3 Power Control with Traffic Considerations

4.3.1 Interference as a Normal Random Process

In Subsection 3.5, Lemma 9, we found that with interference, $I(t)$, modeled as a Normal random process, and with the mean and variance of $I(t)$ upper-bounded by E' and V' respectively, it is sufficient to have $E' + h'\sqrt{2V'} \leq \eta$ ($\text{erfc}(h') = 2\frac{\epsilon}{\Pi}$) in order to have $P_{exc} \leq \epsilon$ where Π is the probability of the primary node being in receiving mode.

Comparing (3.54) and (3.56), with (4.1) and (4.2), we can see that

$$\begin{aligned}E' &= \Delta E, \\ V' &= \Delta V.\end{aligned}\tag{4.20}$$

The results found in Subsections 4.1.1 and 4.1.3, for constant and distance-dependent power control strategies can then be applied with $K_1, K_2, K'_1, \dots, K'_5$ multiplied by Δ .

4.3.2 Sum of Normal and Log-normal Assumption

Comparing equations (3.58) and (3.59) with (3.17) and (3.18), we can see that the same fixed and distance-dependent power control strategies work for this case as well. We can still set $P_{S,i} = p_1$, $1 \leq i \leq N$.

For power control with fixed power levels (i.e., $P_{S,i} = p_2$, $i \geq N + 1$), using (3.58), we have

$$\begin{aligned} \acute{\mu}_2 &= \frac{\Delta E\{\xi\} p_2}{\lambda_c^{\alpha/2}} (\zeta(-\alpha/2) - \sum_{i=1}^N i^{\alpha/2}) \\ &= \Delta \mu_2, \end{aligned} \tag{4.21}$$

and

$$\acute{\sigma}_2^2 = \frac{E\{\xi^2\} \Delta - E^2\{\xi\} \Delta^2}{\lambda_c^\alpha} (\zeta(-\alpha) - \sum_{i=1}^N i^\alpha). \tag{4.22}$$

Similarly, for power control with distance-dependent power levels (i.e., $P_{S,i} = ki^\beta$), we have

$$\begin{aligned} \acute{\mu}_2 &= \Delta \mu_2, \\ \acute{\sigma}_2^2 &= \frac{E\{\xi^2\} \Delta - E^2\{\xi\} \Delta^2}{\lambda_c^\alpha} (\zeta(-\alpha/2 - \beta) - \sum_{i=1}^N i^{\alpha+2\beta}) \end{aligned} \tag{4.23}$$

4.4 Simulation Results

We consider the same simulation model and parameters as the one used in Chapter 3. In Figure 4.3, the power levels of the first 50 secondary neighbors of the primary node are found for an arbitrary realization of the node locations for $\alpha = -3$. Two different values

of $\beta = -\alpha/2 - 1.4$ and $\beta = -\alpha/2 - 1.6$ are considered. They both satisfy the condition $\beta < -\alpha/2 - 1$ and respectively correspond to cases where the power levels are respectively increasing/ Decreasing for $n \geq -\lfloor \alpha \rfloor + 1$.

In Figure 4.4, using the power control strategy with constant power levels (denoted by PCcons in the Figure), we have obtained the simulation results for aggregated interference from the secondary network on the primary node versus path loss exponent and for different values of probability of excess interference ($P_{exc} = 0.01, 0.1$ and 0.2).

Figure 4.5 shows the performance of the second power control strategy with distance-dependent power levels. We have considered β in (4.12) to be $-\alpha/2 - 1.1$.

The aggregated interference is always less than η , the maximum acceptable interference in both of the strategies, while the first strategy seems to fluctuate more rapidly versus path loss exponent.

In Figure 4.6, the power levels chosen for the 10000 nearest secondary neighbors of the primary node using distance-dependent power control strategy with traffic consideration has been depicted. As Δ or Π (i.e., the percentage of time that secondary nodes are in transmission mode or the primary node is in reception mod) is decreased, more relaxed power levels will work fine to satisfy the interference constraint.

In Figure 4.7, probability of excess interference (P_{exc}) is plotted versus path loss exponent for power control strategy with fixed power levels. We have set $p_1 = p_2$ and chose its value such that either bound 1 (equation (3.39)) or bound 2 (equation (3.47)) are satisfied. The (η, ϵ) pair is set to be $(1, 0.01)$. The results show that the interference constrained is always satisfied and probability of excess interference never exceeds the required 0.01 value.

In Figure 4.8, probability of excess interference (P_{exc}) is plotted versus path loss exponent for the power control strategy with distance-dependent power levels. We have assumed $\beta = -\alpha/2 - 1.05$ to satisfy the $\beta < -\alpha/2 - 1$ convergence condition. This leads to increasing power levels for $-\alpha > 2.1$ which includes the range of our simulations. To simplify, we have set $k = p_1 N^{-\beta}$ which leads to the continuity of power levels. p_1 is chosen such that either bound 1 (equation (3.39)) or bound 2 (equation (3.47)) are satisfied. The (η, ϵ) pair

is again set to be $(1, 0.01)$. The results show that the interference constrained is almost always satisfied.

In Figure 4.9, the transmitted power levels are plotted versus path loss exponent. There is a fairly constant gap between the power levels chosen based on bound 1 and those chosen based on bound 2. This implies that the second obtained bound is looser compared to the first one.

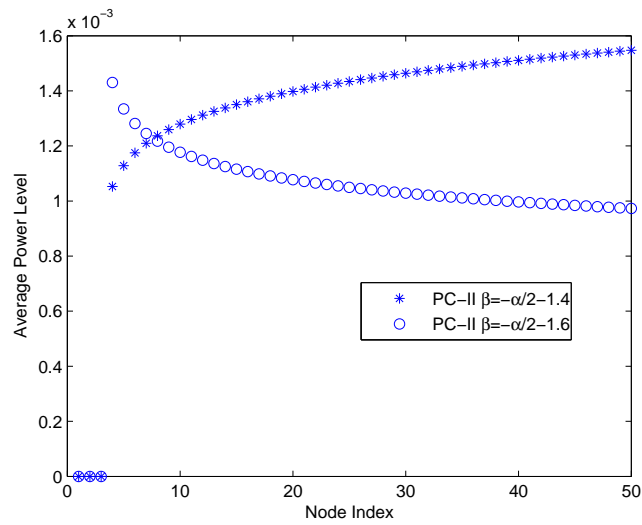


Figure 4.3: Average Power levels of the first 50 secondary neighbors chosen by the second power control strategy ($\alpha = -3, C_2 = 0$).

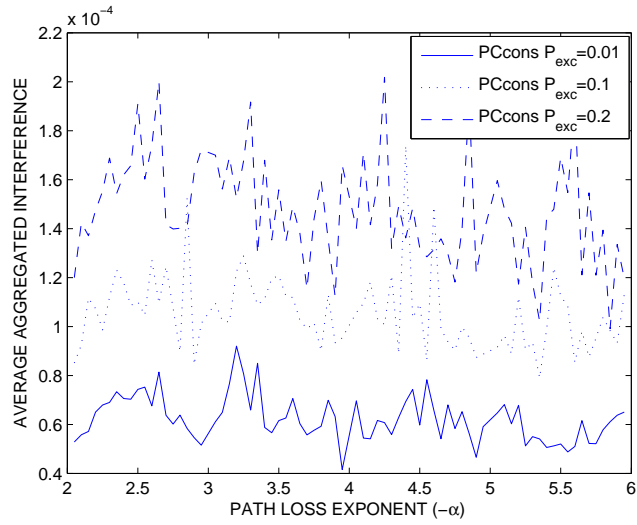


Figure 4.4: Average Aggregated interference from secondary network on the primary node with constant power-level power control strategy ($\eta = 0$ dBm).

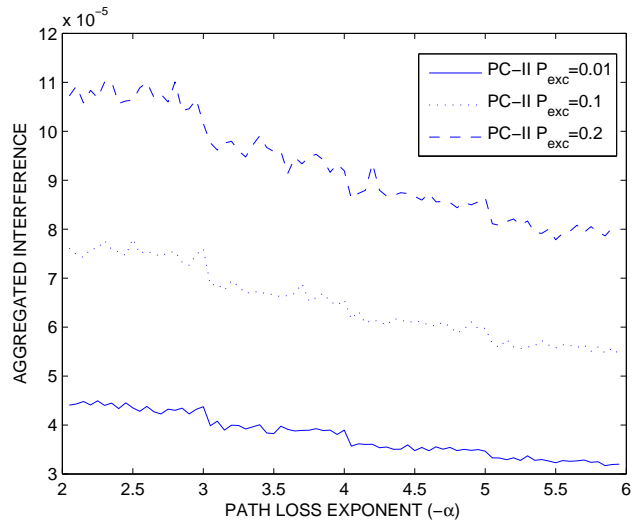


Figure 4.5: Average Aggregated interference from secondary network on the primary node with distance-dependent power-level power control strategy ($\beta = -\alpha/2 - 1.1$, $\eta = 0$ dBm, $C_2 = 0$).

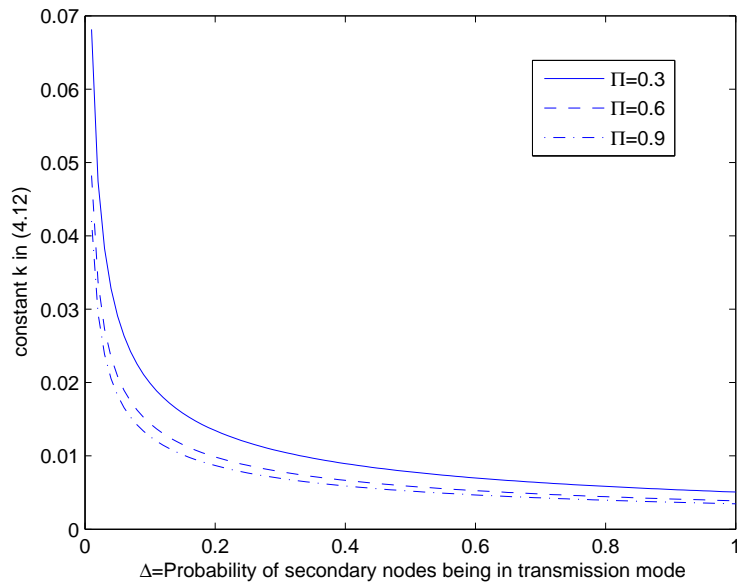


Figure 4.6: constant k in (4.12) when distance-dependent power control strategy is used and for different values of Π and Δ ($\alpha = -3.2, \beta = -\alpha/2 - 1.5 = 0.1, \eta = 0$ dBm, $\epsilon = 0.1, C_2 = 0$).

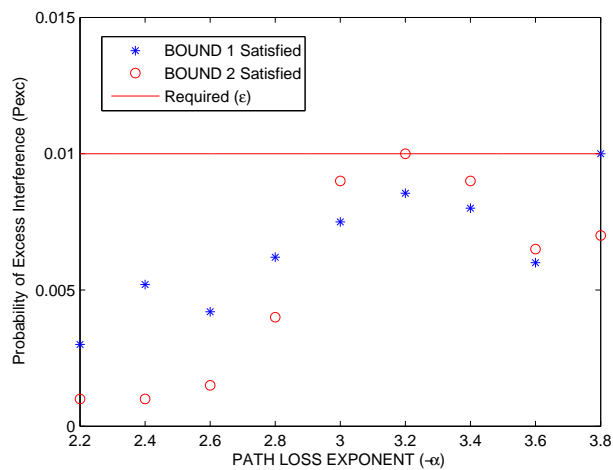


Figure 4.7: P_{exc} vs. Path Loss Exponent for power control strategy with fixed power levels. $p_1 = p_2$ are chosen such that Bound 1 or Bound 2 are satisfied. The threshold for P_{exc} , (i.e., ϵ) is set to 0.01 and $\eta = 1 \sim 0$ dBW.

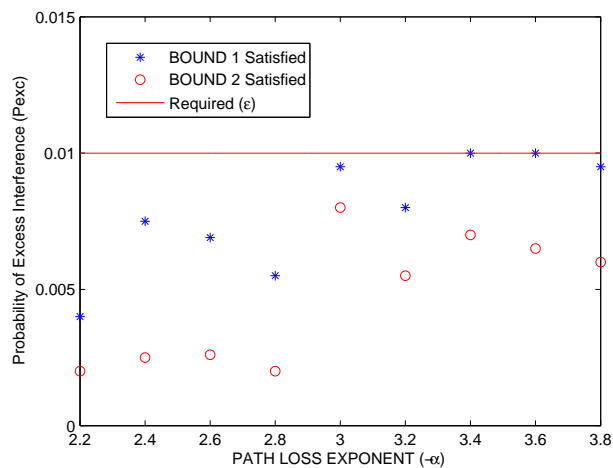


Figure 4.8: P_{exc} vs. Path Loss Exponent for power control strategy with distance-dependent power levels. We have set $\beta = -\alpha/2 - 1.05$ (increasing power levels), and $k = p_1 N^{-\beta}$. p_1 is chosen such that Bound 1 or Bound 2 are satisfied.

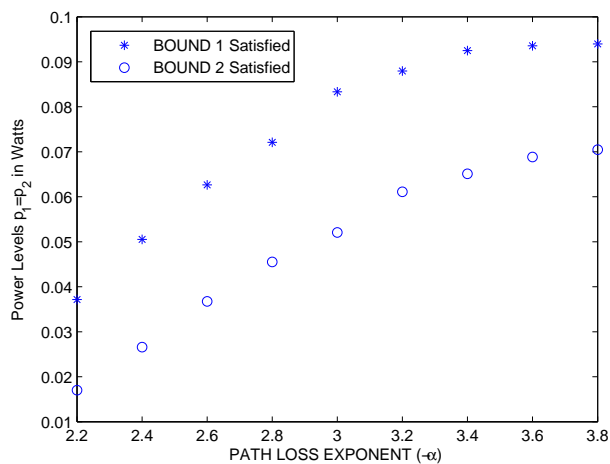


Figure 4.9: Transmitted power level vs. Path Loss Exponent for power control strategy with fixed power levels ($p_1 = p_2$). $p_1 = p_2$ is chosen such that Bound 1 or Bound 2 are satisfied.

Chapter 5: Achievable Throughput in Power-Constrained Cognitive Wireless Networks

In Chapter 4, we proposed power control strategies for the secondary network for its safe operation alongside with the primary network. For this purpose, the secondary neighbors of a primary receiver impose constraints on their transmit power levels such that the probability that the aggregated interference from secondary network is more than some threshold is less than some given value. In this chapter, we answer the question: Given that the secondary nodes have imposed upper limits on their transmit power levels, what is the lower bound of achievable throughput by secondary nodes? Although we answer this question in the context of a cognitive wireless network, the way we have approached the problem, by using the statistical properties of distances, obtained in Chapter 2, to characterize the interference is also applicable to an ordinary power-constrained uniformly random wireless network and has not been used in the literature, to the best of our knowledge.

5.1 Achievable Throughput

The throughput attained by j th nearest secondary neighbor of the primary node when it forwards data to its k th nearest secondary neighbor is:

$$C_{jk} = \log_2 \left(1 + \frac{\xi_{jk} P_{S,j} r_{jk}^\alpha}{\sum_{i=1, i \neq j}^{\infty} \xi_{ijk} P_{S,i} d_{ijk}^\alpha + I_{PS}} \right), \quad (5.1)$$

where following notations apply:

$P_{S,i}$: Transmitted power level for the i th nearest secondary neighbor of a primary node.

I_{PS} : Interference from the primary network

d_{ijk} and r_{jk} are as defined in Figure 2-1, and ξ_{ijk} and ξ_{jk} are the corresponding shadow fading components. We assume that they are σ_s dB log-normal shadowing and all have the same statistics. We also assume that shadowing components are independent from each other and from d_{ijk} and r_{jk} .

We rewrite (4.1) as

$$C_{jk} = \log_2\left(1 + \frac{x_2}{a + x_1}\right) = \log_2\left(1 + \frac{1}{\frac{a+x_1}{x_2}}\right), \quad (5.2)$$

where

$$a \triangleq I_{PS}, \quad x_2 \triangleq \xi_{jjk} P_{S,j} r_{jk}^\alpha, \quad x_1 \triangleq \sum_{i=1, i \neq j} \xi_{ijk} P_{S,i} d_{ijk}^\alpha.$$

The function $f(X) = \log_2(1 + \frac{1}{X})$ is convex for $X > 0$ and, therefore, C_{jk} is convex in $\frac{a+x_1}{x_2}$. We can use Jensen's inequality to write

$$E\{C_{jk}\} \geq \log_2\left(1 + \frac{1}{E\{\frac{a+x_1}{x_2}\}}\right). \quad (5.3)$$

We have

$$E\left\{\frac{a+x_1}{x_2}\right\} = aE\{x_2^{-1}\} + E\{x_1 x_2^{-1}\}. \quad (5.4)$$

Using Cauchy-Schwartz inequality,

$$E\left\{\frac{a+x_1}{x_2}\right\} \leq aE\{x_2^{-1}\} + \sqrt{E\{x_1^2\}E\{x_2^{-2}\}}.$$

So (5.3) can be written as

$$E\{C_{jk}\} \geq \log_2\left(1 + \frac{1}{aE\{x_2^{-1}\} + \sqrt{E\{x_1^2\}E\{x_2^{-2}\}}}\right). \quad (5.5)$$

We have

$$E\{x_2^{-1}\} = \frac{1}{P_j} E\{\xi^{-1}\} E\{r_{jk}^{-\alpha}\}$$

$$E\{x_2^{-2}\} = \frac{1}{P_j^2} E\{\xi^{-2}\} E\{r_{jk}^{-2\alpha}\}$$

and

$$E\{x_1^2\} = \sum_{i=1, i \neq j}^{\infty} \sum_{l=1, l \neq j} E\{\xi_{ijk} \xi_{ljk}\} P_i P_l E\{d_{ijk}^{\alpha} d_{ljk}^{\alpha}\}$$

$$= \sum_{i=1, i \neq j}^{\infty} E\{\xi_{ijk}^2\} P_i^2 E\{d_{ijk}^{2\alpha}\} + \sum_{i=1, i \neq j}^{\infty} \sum_{l=1, l \neq j, i}^{\infty} E\{\xi_{ijk} \xi_{ljk}\} P_i P_l E\{d_{ijk}^{2\alpha} d_{ljk}^{2\alpha}\} \quad (5.6)$$

Using Cauchy-Schwartz inequality we have

$$E\{d_{ijk}^{\alpha} d_{ljk}^{\alpha}\} \leq \sqrt{E\{d_{ijk}^{2\alpha}\} E\{d_{ljk}^{2\alpha}\}}, \quad (5.7)$$

and

$$E\{x_1^2\} \leq \sum_{i=1, i \neq j}^{\infty} E\{\xi_{ijk}^2\} P_i^2 E\{d_{ijk}^{2\alpha}\} + E^2\{\xi\} \left(\sum_{i=1, i \neq j}^{\infty} P_i \sqrt{E\{d_{ijk}^{2\alpha}\}} \right)^2. \quad (5.8)$$

Using above equalities and inequalities

$$E\{C_{jk}\} \geq \log_2 \left(1 + \frac{P_j}{Q_{jk}} \right) \quad (5.9)$$

where

$$\begin{aligned}
Q_{jk} &\triangleq I_{PS} E\{\xi^{-1}\} E\{r_{jk}^{-\alpha}\} \\
&+ E\{\xi\} \sqrt{E\{\xi^{-2}\}} \sqrt{E\{r_{jk}^{-2\alpha}\}} \left[E\{\xi^2\} \sum_{i=1, i \neq j}^{\infty} P_{S,i}^2 E\{d_{ijk}^{2\alpha}\} + E^2\{\xi\} \left(\sum_{i=1, i \neq j}^{\infty} P_{S,i} \sqrt{E\{d_{ijk}^{2\alpha}\}} \right)^2 \right]^{1/2}.
\end{aligned} \tag{5.10}$$

For a zero-mean log-normal distribution, we have

$$E\{\xi^{-1}\} = E\{\xi\} = e^{\sigma_s^2/2} \quad \text{and} \quad E\{\xi^{-2}\} = E\{\xi^2\} = e^{2\sigma_s^2},$$

where $\sigma_S = \sigma_s \frac{\ln 10}{10}$. $E\{r_{jk}^\alpha\}$ and $E\{d_{ijk}^\alpha\}$ were found in Lemmas 4 and 5 in Chapter 2 respectively.

5.2 Forwarding Strategy in the Secondary Network

In (5.1), we defined the throughput of j th nearest secondary neighbor of a primary neighbor, assuming that it forwards its data to its k th nearest secondary neighbor. The choice of k , depends on what kind of forwarding strategy is used in the secondary network. In this section, we consider different forwarding strategies for the secondary nodes and find the achievable throughput by employing each strategy.

5.2.1 Nearest Neighbor Forwarding

In this case, each secondary node is assumed to forward its data to its nearest secondary neighbor, in other words, we have $k = 1$, and

$$C_j = C_{j1} \tag{5.11}$$

5.2.2 Forwarding based on a distribution

In this case, a secondary node forwards its data to one of its K th nearest neighbors with probability $p(k)$ given by a probability distribution. We can consider distributions tilted toward right or left or uniform distribution, which correspond to the cases that further or closer nodes or all of them equally are more likely to be the next-hop node respectively. So we have

$$E\{C_j\} = \sum_{j=1}^K E\{C_{jk}\}p(k) \quad (5.12)$$

Uniform Forwarding

In a large network, we can assume that it is equally likely that a secondary node forwards its data to any of its first K nearest neighbors. So, uniform forwarding is a good model and we will have

$$E\{C_j\} = \frac{1}{K} \sum_{j=1}^K E\{C_{jk}\}. \quad (5.13)$$

5.3 Further Remarks

Although we obtained the achievable throughput for a power-controlled secondary network, the approach can be used for obtaining the capacity in power-constrained random networks. There have been few attempts in obtaining the throughput capacity of power-constrained random ad hoc networks (for example see [42] and [43]). Previous attempts do not consider interference characterization using the statistical properties of distances. Furthermore, a uniform power constraint is imposed upon nodes, whereas in our analysis, we have considered both constant and distance-dependent power levels.

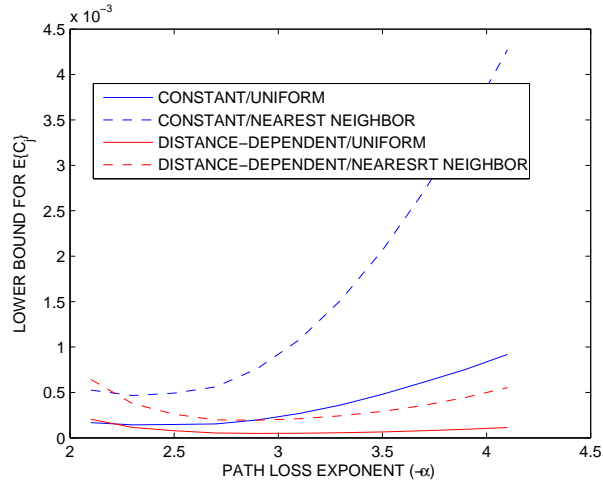


Figure 5.1: Lower-bound for $E\{C_j\}$, $j = 50$, versus path loss exponent, for constant and distance-dependent power control strategies and for uniform and nearest neighbor forwarding.

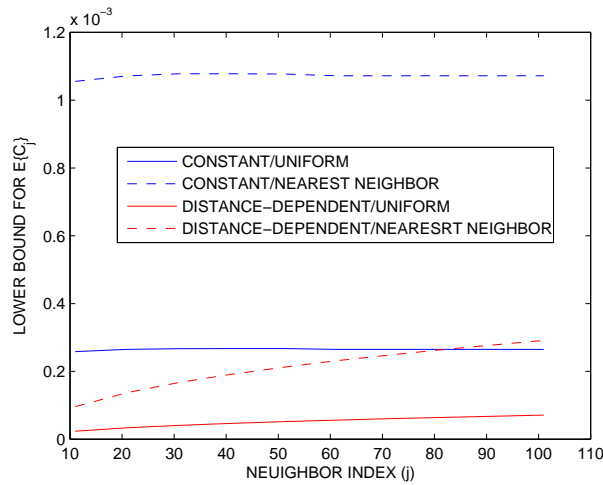


Figure 5.2: Lower-bound for $E\{C_j\}$, versus j ($10 < j \leq 100$ and $\alpha = -3.1$) for constant and distance-dependent power control strategies and for uniform and nearest neighbor forwarding.

5.4 Simulation Results

In Figure 5.1 we have plotted the lower bounds for $E\{C_j\}$ for $j = 50$. We assume that $I_{PS} = -30$ dBm and $K = 10$ in the uniform routing. We have plotted the achievable throughput for both nearest-neighbor and uniform forwarding. We are considering the secondary network to use the constant or distance-dependent power control strategies. For the distance-dependent case, we are considering $\beta = -\alpha/2 - 1.1$. In both cases, we have set the probability of excess interference, ϵ , equal to 0.01. The dashed lines are for the nearest neighbor forwarding and the solid lines are for uniform forwarding. As we mentioned earlier the result for uniform forwarding is more realistic in a large wireless network. It can be seen in the figure that the achievable throughput behaves like a convex function with respect to the $-\alpha$ (i.e., path loss exponent) with the minimum in all of the cases at around $-\alpha = 3$ and for $-\alpha > 3$, the achievable throughput is monotonically increasing.

In Figure 5.2 we have plotted the achievable throughput versus the index of the secondary neighbors. We again assume that $I_{PS} = -30$ dBm and $K = 10$ in the uniform forwarding and we have plotted for both nearest-neighbor and uniform forwarding while the secondary network uses the constant or distance-dependent power control strategies. We consider a path loss exponent of 3.1. The results show that for constant power control strategy, the achievable throughput is relatively constant with respect to node index, whereas for distance-dependent strategy (in this case, for $\alpha = -3.1$ and $\beta = -\alpha/2 - 1.1$, the power levels will be increasing with distance, see (4.12)), the achievable throughput will increase with node index. The nodes farther from the primary node (i.e., nodes with higher index), are prone to receive more interference as they are closer to nodes with higher allowable power levels. On the other hand, they can transmit at higher power levels. The results show that the effect of higher transmit power is dominant and has more effect than the higher received interference, and the achievable throughput increases with the node index.

Chapter 6: Summary, Conclusions, and Future Work

6.1 Summary

Coexistence of wireless networks seems to be the way out of the current spectrum scarcity dilemma. Advances in wireless communications and the introduction of concepts like cognitive radio and cognitive wireless networks, has turned the spectrum sharing among multiple systems from an idea into a possibility.

Interference protection has always been the major issue in a multi-user communications scenario. In the context of coexisting wireless networks, strict policies are required to protect the primary licensed network against the interference coming from secondary unlicensed network. Therefore, the situation is more critical, as the unlicensed wireless network carries all the responsibility to avoid the interference on the primary licensed users.

In such networks, a new type of interference, i.e., inter-system interference comes into the picture. The regulatory policy can be expressed in terms of a constraint on the aggregate interference from secondary network on the primary users. Implementation of cognitive wireless networks requires a model translating the regulatory constraint on the aggregate interference to the system- and device-level design parameters.

In this direction, we need a model for interference whose parameters can be adjusted by tuning the degrees of freedom available for individual devices. In Chapter 2, we consider a spatial bivariate Poisson model for the coexisting wireless networks. To obtain a model for interference, we first need to have a characterization of internodal distances in such processes. We obtain analytical results for the real moments of these distances and find some useful results for the properties of such distances.

Using the results obtained in Chapter 2, we consider two different models for the aggregate interference on a primary node. The first model is found assuming that central limit

theorem can be applied to model the interference as a Gaussian random variable. Upper bounds are obtained for mean and variance of interference. The second model is found by considering the interference as sum of a Normal and Log-normal random variables. Two upper bounds are obtained for the CCDF of interference. In both cases, the parameters of the models are shown to be adjustable by the power levels chosen by secondary users. Using these models, power control strategies are obtained in Chapter 4 to satisfy the interference constraint at the primary node.

In Chapter 5, considering the power-controlled secondary network, and using the statistical properties of distances found in Chapter 2, a lower bound is found for the throughput of secondary nodes which depends on the forwarding strategy used in secondary network.

6.2 Conclusions

Stochastic geometry and spatial point processes are powerful mathematical tools for modeling random networks. While Poisson model is long known to be a simple mathematically tractable approach, the use of bivariate version of this process is shown to be a suitable model for two-type correlated random networks, e.g., cognitive wireless networks.

Due to the random locations of nodes as well as the random propagation channel, the aggregate secondary interference at a primary node has a statistical nature and a statistical model is required to be able to characterize the interference and subsequently satisfy the interference constraint at the primary nodes.

The achievable throughput in power-constrained random networks has been considered in the literature recently. We use the statistical properties of distances to characterize the interference and thereby the achievable throughput in secondary networks. This approach has not been considered in the literature to the best of our knowledge.

6.3 Future Work

The model considered for the cognitive wireless network in this dissertation is based on the underlay approach. To model the aggregate secondary interference, it is either considered that the primary receiver and secondary transmitter are always active (i.e., in transmission and reception modes respectively) or a statistical model for primary and secondary traffic is considered. The model does not consider spectrum sensing and detection of the activity of primary receiver. This can be considered as an extension, where sensing can be done using primary beacon signals and can be performed either individually by secondary nodes or using cooperative sensing [44].

In Chapter 3, we considered a simple M/M/1/1 traffic model. As another future work, we might consider more sophisticated and perhaps non-stationary traffic models. Since the traffic is stochastic and time-varying, we might consider that power levels also be determined dynamically and as a reaction to traffic levels.

In Chapter 5, we obtained the achievable throughput in the power constrained secondary network. Recently, some work is done to find the scaling laws of the throughput in secondary wireless networks (i.e., how the achievable throughput of a network scales with the number of nodes)[45]. As an extension, we can consider the throughput in the primary and secondary networks jointly to obtain analytical results as how the throughput in these networks relate and find tradeoffs and design benchmarks.

Bibliography

Bibliography

- [1] FCC Spectrum Policy Task Force, "Report of the spectrum efficiency working group," Nov. 2002. [Online]. Available: <http://www.fcc.gov/sptf/reports.html>
- [2] A. Goldsmith, S. A. Jafar, I. maric and S. Srinivasa, "Breaking Spectrum Gridlock with Cognitive Radios: An Information Theoretic Perspective," *To appear in Proceedings of IEEE*.
- [3] J. M. Peha, "Approaches to Spectrum Sharing," *IEEE Communications Magazine*, vol. 43, no. 2, pp. 10-12, Feb. 2005.
- [4] Proceedings of *IEEE Symposium on New Frontiers in Dynamic Spectrum Access Networks (DySpan)* 2005.
- [5] J. Mitola, G.Q. Maguire, "Cognitive radio: making software radios more personal," *IEEE personal Communications*, vol.6, no.4, pp. 13-18, Aug. 1999.
- [6] J. Mitola, "The Software radio architecture," *IEEE Communications Magazine*, vol. 33, no. 5, pp. 26-38, May 1995.
- [7] Software Defined Radio Forum: <http://www.sdrforum.org/>
- [8] S. Srinivasa and S. A. Jafar, "The Throughput Potential of Cognitive Radio: A Theoretical Perspective," in *Proceedings of IEEE ACSSC 2006*, pp. 221 - 225, .
- [9] Q. Zhao and B. M. Sadler, "A Survey of Dynamic Spectrum Access," *IEEE Signal Processing Magazine*, vol. 24, no. 3, pp. 79-89, May 2007.
- [10] N. Devroye, P. Mitran and V. Tarokh, "Achievable Rates in Cognitive Radio Channels," *IEEE Trans. Inf. theory*, vol. 52, no. 5, pp. 1813-1827, May 2006.
- [11] M. Costa, "Writing on dirty paper," *IEEE Trans. Information Theory*, vol. 29, no. 3, pp. 439-441, May 1983.
- [12] S. Gel'fand and M. Pinsker, "Coding with Channels with Random Parameters," *Probl. Contr. and Inf. Theory*, vol. 9, no. 1, pp. 19-31, 1980.
- [13] O. Simeone, J. Gambini, Y. Bar-Ness, U. Spagnolini, "Cooperation and Cognitive Radio," in *Proceedings of IEEE ICC 2007*, pp. 6511-6515, June 2007.
- [14] S. A. Jafar and S. Srinivasa, "Capacity Limits of Cognitive Radio with Distributed and Dynamic Spectral Activity," *IEEE JSAC*, vol. 25, no. 3, pp. 529-537, Apr. 2007.

- [15] L. Le and E. Hossain, "Resource Allocation for Spectrum Underlay in Cognitive Radio Networks," *IEEE Trans. Wireless Comm.*, vol. 7, no. 12, Dec. 2008.
- [16] Q. Zhao, L. Tong, A. Swami and Y. Chen, "Decentralized cognitive MAC for opportunistic spectrum access in ad hoc networks: A POMDP framework," *IEEE Journal on Selected Areas in Communications*, vol. 25, no. 3, pp. 589-600, Apr. 2007.
- [17] R. Etkin, A. Parekh and D. Tse, "Spectrum sharing for unlicensed bands," *IEEE Journal on Selected Areas in Communications*, vol. 25, no. 3, pp. 517-528, Apr. 2007.
- [18] H. Islam, L. Ying-chang and H. Anh, "Joint power control and beamforming for cognitive radio networks," *IEEE Trans. Wireless Comm.*, vol.7, no. 7, pp. 2415-2419, July 2008.
- [19] W. Wang, T. Peng, and W. Wang, "Optimal Power Control under Interference Temperature Constraints in Cognitive Radio Network," *Proceedings of IEEE WCNC 2007*, pp. 116-120, March 2007.
- [20] H. T. Lee and Q. Liang, "An Efficient Power Control Scheme for Cognitive Radios," in *Proceedings of IEEE WCNC 2007*, pp. 2559 - 2563, March 2007.
- [21] L. Qian, X. Li, J. Attia, and Z. Gajic, "Power Control for Cognitive Radio Ad Hoc Networks," in *Proceedings of 15th IEEE Workshop on Local and Metropolitan Area Networks*, pp. 7-12.
- [22] W. Wang, Y. Cui, T. Peng, and W. Wang, "Noncooperative Power Control Game with Exponential Pricing for Cognitive Radio Network," in *Proceedings of IEEE VTC 2007-Spring* pp. 3125 - 3129, April 2007.
- [23] Y.M. Shobowale, K.A. Hamdi, "Interference Characterization in the Unlicensed Band," *IEEE Comm. Letters*, vol. 10, no. 6, June 2006.
- [24] E. S. Sousa, "The performance of a FH/MFSK link in a Poisson field of interferers, in *Proceedings of Int. Conf. Commun.SUPERCOMM/ICC'90* , vol. 3, pp. 1246 - 1250, April 1990.
- [25] A. Babaei and B. Jabbari, "Internodal Distance Distribution and Power Control for Coexisting Radio Networks," *Proceedings of IEEE Globecom 2008*, pp. 3039-3043, Dec. 2008.
- [26] A. Ghasemi, "Statistical Characterization of Interference in Cognitive Radio Networks," *Proceedings of PIMRC 2008*, pp. 1-6, Sept. 2008.
- [27] A. Babaei and B. Jabbari, "Interference Modeling and Power Control in Cognitive Wireless Networks," Submitted for publication.
- [28] D. Stoyan, W. S. Kendall, and J. Mecke, *Stochastic Geometry and its Applications*, 2nd Edition, Jhon Wiley, 1985.
- [29] H. Takagi and L. Kleinrock, "Optimal Transmission Ranges for Randomly Distributed Packet Radio Terminals" *IEEE Trans. Commun.*, vol. 32, no. 3, pp. 246-257, Mar. 1984.

- [30] M. Haenggi, "On Distances in Uniformly Random Networks," *IEEE Trans. Inf. Theory*, vol. 51, no. 10, pp. 3584-3586, Oct. 2005.
- [31] S. Srinivasa, M. Haenggi, "Distance Distributions in Finite Uniformly Random Networks: Theory and Applications," Submitted to *IEEE Trans. on Vehicular Technology*.
- [32] A. Babaei and B. Jabbari, "On Distances in Correlated Random Networks," Submitted for publication.
- [33] A. Babaei and B. Jabbari, "Distance Distribution and Power Control Strategies for Coexisting Wireless Networks," Submitted for publication.
- [34] Francois Baccelli, Maurice Klein, Marc Lebourges and Sergei Zuyev, "Stochastic geometry and architecture of communication networks," *Journal of Telecommunication Systems*, Springer Netherlands, vol. 7, pp. 209-227, 1995.
- [35] T. C. Brown, B. W. Silverman, and R. K. Milne, "A Class of Two-Type Point Processes", *Zeitschrift fur Wahrscheinlichkeitstheorie und verwandte Gebiete*, vol. 58, pp. 299-308, 1981.
- [36] J. E. Palohimo, "A Spatial Bivariate Poisson Distribution," *Biometrika* vol. 59, no. 2, pp. 489-492, 1972.
- [37] M. Abramowitz and I. Stegun, *Handbook of Mathematical Functions*, Dover, 1972.
- [38] A. papoulis, S. U. Pillai, *Probability, Random Variables and Stochastic Processes*, 4th Edition, McGraw Hill, 2002.
- [39] M. Pratesi, F. Santucci, and F. Graziosi, "Generalized Moment Matching for the Linear Combination of Lognormal RVs: Application to Outage Analysis in Wireless Systems," *IEEE Trans. Wireless Comm.*, vol. 5, no. 5, pp. 1122-1132, May 2006.
- [40] W. Gautschi, "Some Elementary Inequalities Relating to the Gamma and Incomplete Gamma Function," *J. Math. Phys.*, vol. 38, pp. 77-81, 1959.
- [41] H. M. Edwards, *Riemann's Zeta Function*, Academic Press, 1974.
- [42] M. Vu, N. Devroye and V. Tarokh, "An Overview of Scaling Laws in Ad Hoc and Cognitive Radio Networks," *Wireless Personal Communications*, vol.45, no. 3, pp. 343-354, May 2008.
- [43] R. Negi and A. Rajeswaran, "Capacity of power constrained Ad-hoc Networks," in *Proceedings of IEEE INFOCOM 2004*, pp. 443-453, March 2004.
- [44] A. Ghasemi and E. S. Sousa, "Spectrum sensing in cognitive radio networks: The cooperation-processing tradeoff," *Wiley Wireless Communications and Mobile Computing*, vol. 7, no. 9, pp. 1049-1060, Nov. 2007.
- [45] X. Tang and Y. Hua, "Capacity of Ultra-wideband Power-constrained ad hoc Networks," *IEEE Trans. Inf. Theory*, vol. 54, no. 2, pp. 916 - 920, Feb. 2008.
- [46] S. Haykin, "Cognitive radio: brain-empowered wireless communications," *IEEE Journal on Selected Areas in Communications*, vol. 23, no. 2, pp. 201-220, Feb. 2005.

[47] A. F. Karr, *Point Processes and Their Statistical Inference*, CRC press, 1999.

Curriculum Vitae

Alireza Babaei was born in Tonekabon, Iran in 1981. He received his BS and MS degrees in Electrical Engineering from K. N. Toosi University of Technology and Iran University of Science and Technology in Tehran, Iran in 2003 and 2005 respectively. Prior to starting his PhD program in 2006, he worked as a lecturer and taught courses in communications and digital logic. His area of active research is on stochastic processes, modeling and performance analysis of wireless networks and mathematical programming.